DESIGN, DEVELOPMENT AND TESTING OF AN INNOVATIVE LOW COST MAGNETO RHEOLOGICAL FLUID BASED DYNAMIC VIBRATION ABSORBER

Project Report

Submitted in partial fulfilment of the requirements for the award of the degree of

Bachelor of Technology
in
Mechanical Engineering

by

AKSHAY KUMAR (*Roll No.*: **B170887ME**)
GANGA NAIR B (*Roll No.*: **B180452ME**)
NATHAN JOB ANTONY (*Roll No.*:**B180497ME)**
SEBIN SABU MATHEW **(***Roll No.***:B180838ME)**

Department of Mechanical Engineering
NATIONAL INSTITUTE OF TECHNOLOGY CALICUT

April 2022

CERTIFICATE

This is to certify that the report entitled "**DESIGN, DEVELOPMENT AND TESTING OF AN INNOVATIVE LOW-COST MAGNETO RHEOLOGICAL FLUID BASED DYNAMIC VIBRATION ABSORBER**" is a bonafide record of the **Project** done by), **AKSHAY KUMAR (*Roll No.*: B170887ME**), **GANGA NAIR B. (*Roll No.*: B180452ME, NATHAN JOB ANTONY (*Roll No.*:B180497ME**) and **SEBIN SABU MATHEW (*Roll No.*:B180838ME)** under our supervision, in partial fulfilment of the requirements for the award of the degree of **Bachelor of Technology** in **Mechanical Engineering** from **National Institute of Technology Calicut**, and this work has not been submitted elsewhere for the award of a degree.

Dr. JAGADEESHA T
(Guide)
Asst. Professor
Dept. of Mechanical Engineering

Dr. G VARAPRASAD
(Guide)
Asst. Professor
Dept. of Mechanical Engineering

Professor & Head
Dept. of Mechanical Engineering

Place: NIT Calicut
Date: 30 April 2022

ACKNOWLEDGEMENT

Firstly, we would like to thank our project guide, Dr. Jagadeesha T, for giving us this wonderful opportunity to study and engage in research at NIT Calicut. We will be ever grateful for all his support and advice. We would also like to express our sincere gratitude to our co-guide, Dr. G Varaprasad.

We are grateful to the Mechanical Department of NIT Calicut for giving us the opportunity to work on this project. We would like to thank the HOD, Dr. C Muraleedharan, for his kind and earnest support of our project. We are especially grateful to the faculty members who went out of their way to support us. Dr. Ashesh Saha and Dr. A. P. Sudheer. Many thanks are due to Mr. Amit Malghol for helping us out with the experimentation, accommodating us in his lab, and giving insightful advice in many situations otherwise. We also thank Ambudan Sir for his insights into control systems and their design. To all members of the Central Workshop, Production lab and Fluid lab, thank you for welcoming us into the labs and showing your willingness to help us with the challenges faced during fabrication when we needed it.

We would also like to thank the Dean of Research and Consultancy, Dr V Madhusudanan Pillai and the professors in the panel, Dr. A Shaija, Dr. Sameer and Dr. Sandhya Rani, for giving us the chance to be a part of the UG Innovative project funding program and for the financial aid and support provided through the program.

AKSHAY KUMAR
GANGA NAIR B.
NATHAN JOB ANTONY
SEBIN SABU MATHEW

ABSTRACT

Tackling vibration and problems caused by it has been a significant area of study in engineering, and solutions, including dampers, vibration absorbers, isolators etc., have been developed and utilised for long. Traditional passive vibration absorption systems can attenuate vibrations of a particular frequency, but many applications today require protection from vibrations over a larger range of frequencies with minimum energy consumption and complexity.

Our project aims to develop a Dynamic Vibration Absorber that can be tuned to absorb the vibration of any frequency by utilising Magneto-Rheological Fluids (MR Fluids). MR Fluids are fluids whose rheological properties can be varied through a magnetic field. MR Dampers have long been used in many applications, including in vehicles to achieve better ride control.

MR Dampers, when used in semi-active vibration absorbers, can tune it, by varying the damper characteristics, to absorb the incident vibration, whatever its frequency. This DVA is designed to be semi-active as it will provide absorption over a wide range of vibration frequencies without the energy consumption, cost or maintenance required for active vibration absorption.

Keywords: MR Dampers, Vibration Absorption, MR Fluids, Dynamic vibration Absorbers

CONTENTS

LIST OF SYMBOLS

μ_{app}	Apparent Viscosity
μ_p	Plastic Viscosity
μ	Mass ratio
Re	Reynolds Number
x	Displacement of Primary Mass
k	Stiffness of primary mass
m_1	Primary Mass
m_2	Secondary Mass
t	Time (s)
ρ	Density
τ_y	Yield Stress
$\dot{\gamma}$	Shear rate
T	Absolute temperature (K)
B	Magnetic Flux Density
H	Magnetic Field Intensity

Subscripts and Superscripts

A_{ij}	Row *i* and column *j* element of matrix/tensor *A*
x_i	Related to the i th body

LIST OF FIGURES

LIST OF TABLES

CHAPTER 1

INTRODUCTION

Vibrations are periodic or random oscillations that occur about an equilibrium point. Vibrations occur as an undesirable effect in many engineering applications like heavy machinery and tall structures. Many methods have been formulated to control and minimize the effects of vibration, including dampers, vibration absorbers, isolators etc. While dampers attempt to dissipate vibrational energy quickly and thus decrease its amplitude, vibration absorbers try to restrict vibration to a secondary system such that it does not affect the crucial components.

A passive vibration absorber suppresses vibrations from a source when tuned to the right frequency. However, if the exciting frequency varies, the vibration of the entire system may increase significantly. This problem arises during the operation of wind turbines. Since wind conditions continually change, it is not possible to create a traditional tuned DVA system for a wind turbine. The changes in wind speed and wind direction can cause continually changing vibrations. This problem is also evident in large pumps, where the nature of fluids causes vibrations with varying properties. Thus, an essential and desirable characteristic of vibration control devices is the ability to be tuned to a wide range of frequencies. This can be achieved using active or semi-active vibration absorbers.

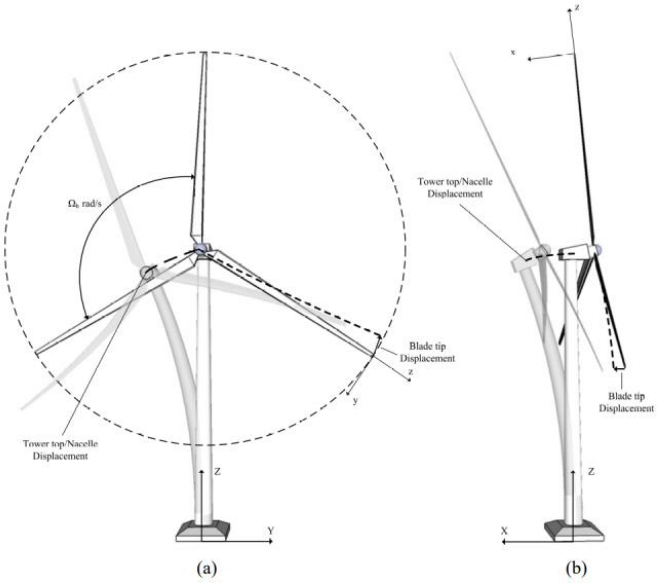

Fig 1.1. The vibration of Wind turbine (a) in plane and (b) out of plane

While active vibration absorbers are effective in eliminating vibrations to a high level of accuracy, which may be of use in highly sensitive equipment, most applications require a more energy-efficient and simpler set-up that can effectively reduce the damage vibrations may cause. Semi-active vibration absorbers are effective and dependable on this front. They consume less power, can be tuned to a wide range of frequencies and can also behave as a passive component in case of loss of power.

The paths to attain a feasible semi-active absorber are few. This includes utilizing systems with varying damping ratios, varying stiffness and varying mass distributions. The control of these variable properties should be easy, fast and should consume minimum power. Smart materials are ideal candidates here.

1.1 INTRODUCTION

The work proposed, focuses on the control of periodic vibration with the help of smart materials, specifically Magneto-Rheological fluid, to achieve variable stiffness/damping properties. MR fluids are a class of fluids whose rheological properties can be changed by subjecting the fluid to a magnetic field. It consists of micron-sized, magnetically polarizable particles dispersed in a carrier medium such as mineral or silicone oil. Thus a semi-active vibration absorber that can absorb vibrations over a large range of frequencies with low power consumption and low response time can be developed.

1.2 OBJECTIVES

This proposed work aims to design and develop an experimental set-up for vibration control magneto rheological fluid based dynamic vibration absorber (DVA). The process involves the development of a realistic dynamic model of an MR Damper, which is to be used as the primary component in the DVA.

- **Design of complete DVA** with vibration absorption over a wide range of vibration profiles, optimised secondary mass and stiffness values for different applications
- **Optimised control system for MR Damper,** thus eliminating the need for manual input or supervision.

- **Innovations for improved performance:** Implementing Energy harvesting technology to reduce energy consumption, agitating mechanism to improve stability of MR Fluid
- **Analysis of experimental data** to optimise the DVA, validate mathematical model and design.

1.3 PROBLEM OUTLINE

Vibration has undesirable effects in most engineering systems. It can cause wastage and damage in many spheres, including:

- Fatigue failure in components due to repeated oscillatory motion
- Loss of accuracy in tasks such as machining
- Malfunctioning of sensitive instruments
- Severe damage due to resonance

Therefore vibration control systems are essential in a wide and varied range of fields.

The primary design considerations for a vibration absorber in typical engineering applications would be to create a device that is tuneable over a wide range of frequencies, has quick re-tuning with minimum power consumption, minimum redundant mass, is cheap and easy to design and manufacture.

A system that combines the features of active and passive system dynamic absorbers could have a lot of merit in meeting the above design considerations. These function via algorithms that regulate certain control actions using measured excitation and response in the semi-active system. Such systems potentially offer the reliability of the passive system and adaptability of active systems. At the same time, unlike in the case of an active system, since no energy is inputted directly to the system, the energy required for the control action is much less. The system is also relatively simple to obtain or manufacture.

The semi-active system chosen also has some desirable characteristics. The feasibility of the system depends on its ease of control, response time (rise time and settling time), range of operation, its compatibility to the application (such as rattle space required), stability with respect to changing environment etc. Smart materials, including Magnetorheological Fluid (MRF) and elastomer (MRE), belong to a family of rheological materials that undergo rheological changes under the application of magnetic fields. MR Fluids are used

in dampers which provide continuously and rapidly adjustable yield stress according to the input provided. This is utilized as the major component of the semi-active vibration.

The choice of MR is made over other alternatives such as ER (Electrorheological fluid) due to the following reasons:

- The yield stress of MR fluids is high (compared to ER fluid) (yield stress values more than 80 kPa are easily obtained when a magnetic field is applied). Therefore, the power required is much smaller.
- It can operate at temperatures from — 40 to 150 °C. The yield strength varies only slightly over this range.
- MR fluids can respond to an applied magnetic field within milliseconds. The compliance of a particular device and the rate at which the magnetic field is generated are two key factors affecting the response time.
- MR fluids are not affected by chemical impurities normally produced during manufacturing and use.

Raw materials used to produce MR Fluids are non-toxic and environmentally safe.

1.4 OUTLINE OF REPORT

In this report, we will be displaying and discussing our findings from the work done. Initially, a mathematical model was created for our model and this was used in simulink to create a theoretical model of our system. This had helped us in understanding the feasibility of such a model for our application.

A study was conducted to understand the different MR fluids commercially available and a MR Fluid appropriate for our study was chosen. Then, Comsol was used to understand the dynamics and multiple physics of the fluid in the damper. Magnetic, force and flow analysis was conducted and results obtained from this has helped us in understanding the damper and certain parameters associated with it.

A model for the experimental system was designed using Solidworks. Additionally, certain innovations like an agitator piston and piezoelectric cantilever beam was designed. This model will then be used for fabrication of the model, which will be then used for experimentation.

CHAPTER 2
REVIEW OF LITERATURE

2.1 MR FLUID

The synthesis and characterization of MR fluid has been discussed extensively in literature. Lazareva and Shitik [1] studied the properties of MR fluids that were based on barium, strontium ferrites and iron oxides. The properties of this fluid and their variation with material was studied by Ashour et al. [2]. MR fluid was found to have issues due to sedimentation of magnetic particles which was also included in the study. An attempt was made to optimize the composition of the fluid such that the fluid had the desired properties. In another study, Ashour et al. [3] studied the general composition of MR fluid along with the methods that were used to evaluate the performance of the fluids. There was also an introduction to the fundamental MR devices that exploit the MR effect.

As per the flow morphology of the magneto-rheological fluid, the function of MR Fluid can be described in three modes namely valve mode, shear mode, and squeeze mode (Fig 2.1). Dampers utilize valve mode the most where the magnetic field is placed perpendicularly to the two parallel plates, while the MR fluid flows along the channel direction. Consequently, the magnetized and the resultant chain-like MR fluid obstructs the flow between the two plates. Hence, the damping force (along the channel direction) builds upon the contact surface of the plates. This is understood in Kolekar S and Venkatesh K when they studied the vibration controllability of sandwich structures with smart materials [4].

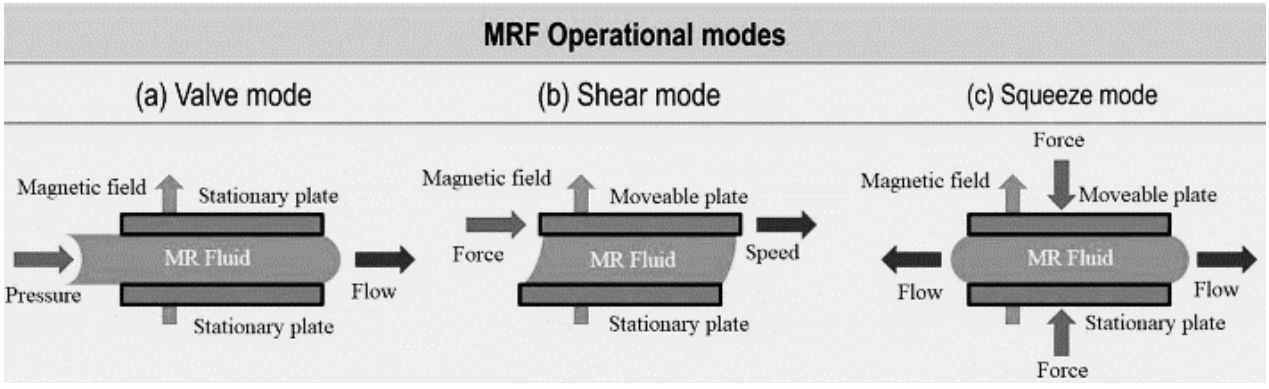

Fig 2.1 Three operational Modes of MR Fluid.

The following studies explored the design of MR fluid devices. Carlson et al. [5] studied the advantages of MR over ER fluid devices in areas such as the yield strength, the required

working volume of fluid, and the required power. The operational modes of the MR fluid were presented along with the linear fluid damper, the rotary brake, and the vibration damper. Kordonsky [6] developed the concept of the MR converter (or valve) and applied the MR converter to create devices such as the MR linear damper, the MR actuator, and the MR seal. Bolter and Janocha [7] examined the rules that should be applied when designing the magnetic circuit for MR devices that are working in the different modes of the MR fluid. They also examined the use of permanent magnets in the design of the magnetic circuit to change the operational point of the MR device.

J. D. Carlson [8,9], affiliated to Lord Corp, filed a patent on the MR fluid damper (Fig 2.2). Here, the damper contained the two key elements, the piston (labelled as 32) and the sleeve (labelled as 20). A mall gap (about 0.5~2 mm) was constructed between the outside wall of the piston and the inside wall of the sleeve to enable the MR fluid to flow. The MR fluid was sealed in the sleeve, and the piston could move along the axis of the sleeve. When the excitation current was supplied by the line (47 and 45), the coil embedded in the piston would generate a magnetic field that passed through the gap and the sleeve and then formed a circular loop. When the current varied, the viscosity of the MR fluid located in the gap changed, thus changing output damping force.

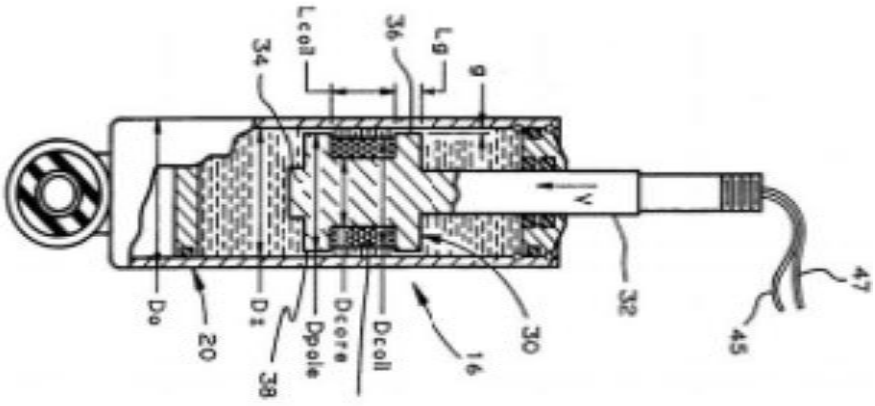

Fig 2.2: Scheme view of damper first developed by Carlson

2.2 VIBRATION CONTROL

Control strategies of MR fluid-based devices are a field of many studies. In 1974 when the semi-active vibration control system of force generator was researched, Karnopp et al. [10] proposed a damping control method called the Skyhook damping control, where the basic

idea was to change the coefficient of damping. A semi-active control algorithm was first proposed by Kamagata et al. [11]. This method further allows switching the current back and forth between several control positions (generally 2–3 control positions) based on different motion conditions.

Yoshida and Dyke [12] identified that there was a linear relationship between the voltage applied in the MR damper and the maximum damping force with a coefficient μ. This relationship ($Vi=\mu\times fc$) was incorporated into the clipped-optimal control method [13] in Pohoryles' and Dufour's work on control algorithms for MR fluid-based vibration control systems.

The study by Margolis [14] examined the effects of using realistic feedback signals when controlling active and semi-active suspension systems. This was an analytical study that suggested several feedback strategies so that the performance can approach the fully active type performance.

Hwang et al. [15] presented a simulation of the dynamic model of the system. The semi-active damper under test was excited according to the computer numerical simulation, and the response of the hardware was measured and fed back to complete the simulation.

Titli et al. [16] compared the designs of semi-active dampers with an optimal controller, sliding mode controller and fuzzy controller. Their performances were tested by simulation on more realistic models, including non-linearities and time delays. Decarlo et al. [17] presented the design of variable structure control systems for a class of multivariable nonlinear time-varying systems. Besides, the paper investigated the applications and developments of this powerful control.

The damping force control performance using the skyhook controller and PID controller were evaluated r in [18]. In this work, the combination of the skyhook and PID controllers was also considered to control the damping force of MR dampers.

It is remarked here that in most MRF and MRE applications, the PID controller has been experimentally realized as presented in [18, 19, 20, 21, 22].

In the study [23], all of the state variables were assumed to be available for designing SMC and directly applied to control the desired damping force. Another study applying SMC to suspension vehicle was presented in [24] in which the observer sliding model was established from the original model, and the saturation function was used instead of the

sign function to prevent the chattering phenomenon. A combination of the fuzzy logic control and sliding mode control was presented in [25, 26] for improvement of robust control performances of MRF rotary damper and MRF mount Kumbhar et al. [27, 28] investigated smart material used as stiffness tuning element in adaptively tuned vibration absorber using shape memory alloy. They also presented a dynamic response of SMA-Magneto-rheological elastomer combined together to act as a smart spring mass damper system. The experimental results compared with analytical results is in good agreement. Jin and Nien [29] presented the adaptive shape control for vibration suppression of a cantilever beam using a piezoelectric damping-modal actuator/sensor.

CHAPTER 3

MATHEMATICAL MODELLING

3.1 MATHEMATICAL MODELLING

3.1.1 Mathematical Model for Dynamic Vibration Absorber

Fig 3.1 shows the schematic diagram for a primary mass system (a simple model for any physical system subjected to excitation) associated with an auxiliary system, the dynamic vibration absorber.

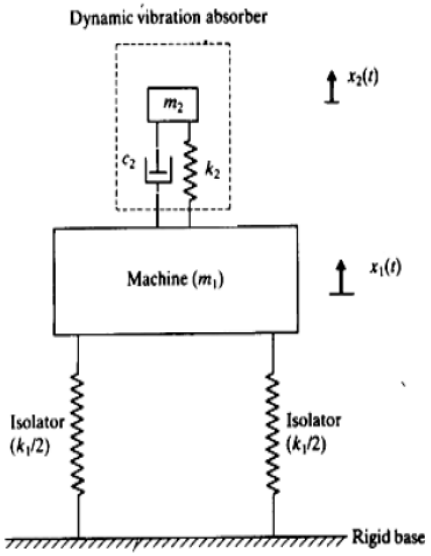

Fig. 3.1. Schematic diagram of primary mass with auxiliary system

At mass m1,

$$m_1\ddot{x}_1 = me\omega^2 sin\omega t \; - \; k_1x_1 - k_2(x_1 - x_2) - f_d \qquad (1)$$

At mass m2,

$$m_2\ddot{x}_2 = k_2(x_1 - x_2) + f_d \qquad (2)$$

Here, x_1 and x_2 are the displacements of primary and auxiliary masses, respectively and f_d is the force provided by the MR damper.

Let's assume the excitation is caused by a unbalanced rotating mass. The amplitude of exciting force due to eccentricity is $F_o = me\omega^2$, where m is the mass of rotating body and e is radial eccentricity of its COM. ω is the frequency of rotation.

Equations 1 and 2 can be rearranged as

$$\ddot{x}_1 = -\left(\frac{k_1+k_2}{m_1}\right)x_1 + \left(\frac{k_2}{m_1}\right)x_2 - \left(\frac{f_d}{m_1}\right) + \left(\frac{me\omega^2}{m_1}\right)sin\omega t \quad (1)$$

$$\ddot{x}_2 = -\left(\frac{k_2}{m_2}\right)x_2 + \left(\frac{k_2}{m_2}\right)x_1 + \left(\frac{f_d}{m_2}\right) \quad (2)$$

This is form is convenient to produce Simulink model later.

3.1.2 Mathematical Model for MR Damper.

Modified Bouc-Wen model

An appropriate mathematical model for the MR damper requires it to be an accurate depiction of such a system, so that the feasibility of MR fluids in DVA's can be assessed. One such model is the modified Bouc Wen hysteresis model, proposed by Ai and Liao. The mechanical model of the MR damper is shown in Fig 3.2

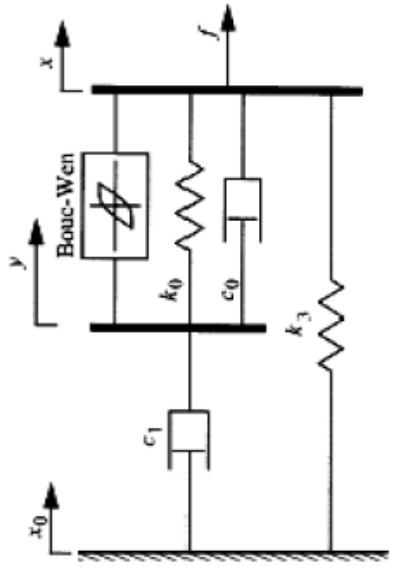

Fig. 3.2. Mechanical model of MR Damper

The equations for this model are as follows:

$$\dot{y} = \frac{1}{c_0 + c_1}[\alpha z + c_0\dot{x} + k_0(x - y)]$$

$$\dot{z} = -\gamma|\dot{x} - \dot{y}|z|z|^{n-1} - \mu(\dot{x} - \dot{y})|z|^n + A(\dot{x} - \dot{y})$$

$$f_d = c_1\dot{y} + k_3(x - x_0) \quad (5)$$

Here, $x_0$is the initial displacement to spring whose stiffness is k_0 (pre-load). It controls the stiffness at large velocities. c_0 is the viscous damping at large velocities and c_1 is a dashpot used to introduce the non-linear roll off observed at low velocities and z is used as a variable to depict the history dependence of applied response. x is the displacement of damper piston.

The relations connecting the model parameters with applied voltage are given below.

$$\alpha = \alpha(u) = \alpha_a + \alpha_b u$$
$$c_1 = c_1(u) = c_{1a} + c_{1b}u$$
$$c_0 = c_0(u) = c_{0a} + c_{0b}u \quad (6)$$

Where u is the output for first order filter, given by

$$\dot{u} = -\eta(u - v) \quad (7)$$

There are 14 parameters $(k_0, c_{0a}, c_{0b}, c_{1a}, c_{1b}, k_3, x_0, \alpha_a, \alpha_b, \mu, \gamma, A, n, \eta)$ present in this model to characterize the MR dampers. The high number of model parameters have increased the complexity of the model which may cause problems in their identification and hence such a model is only used when an accurate depiction is needed.

A Simulink model is developed using equations 1-7, to assess MRDVA responses.

Bingham model

Effects of MR Damper and its force characteristics can be represented in a simpler manner using the Bingham model. This model is a reasonable simplification for most application

including that of dampers used in DVA. The model expresses force as a function of displacement and velocity.

$$F = c_0\dot{x} + k_0 x + \alpha z + f_0$$

Where,

$$z = \tanh(\beta\dot{x} + \delta \times sign(\dot{x}))$$

The parameters vary according to current and therefore, are expressed as a third degree polynomial function of current.

3.2 SIMULINK MODEL

The simulation of the above mentioned mathematical model has been done in MATLAB/SIMULINK. Simulink is a graphical programming environment built on MATLAB for modelling, simulating and analysing systems. This allows us to simulate the model dynamically, observe the response, and obtain the required characteristics. The equations are modelled using integrators and sum blocks, with the parameters represented as constant blocks. The differential equations are solved with embedded MATLAB functions reducing the effort required to code and making the simulation graphical and easy to understand. MATLAB R2020b is utilised for simulation. The solver is ode45 with variable time steps.

3.2.1 MR Damper model – Modified Bouc Wen Model

The modified Bouc Wen model representing the characteristics of MR Damper has been simulated using a Simulink model. x is the input vibration or excitation on the damper and f_d is the force exerted by the damper (output of the model). The voltage given can be controlled as a function or a constant source.

The various equations of the model are simulated as subsystems for ease of understanding. This is explained below:

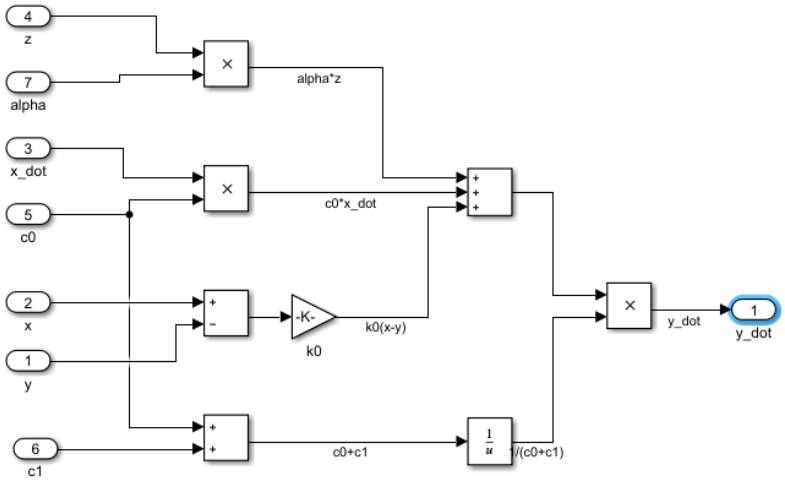

Fig. 3.3. Simulink subsystem representing $\dot{y} = \frac{1}{c_0+c_1}[\alpha z + c_0\dot{x} + k_0(x-y)]$

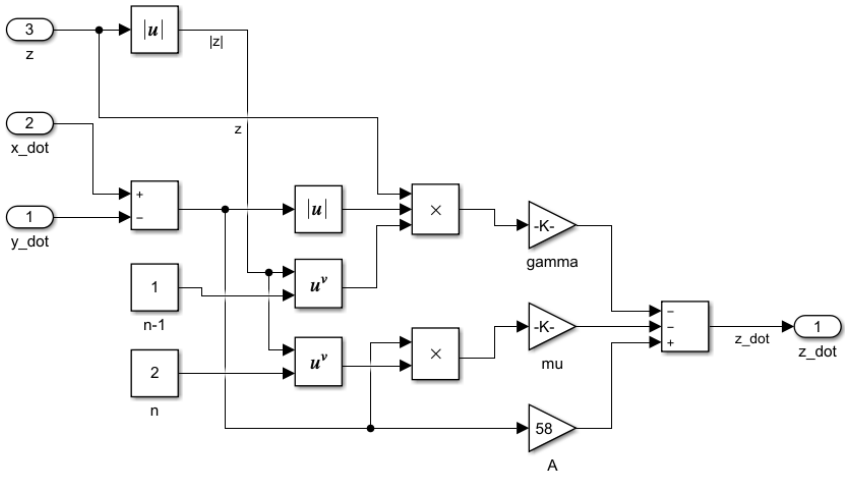

Fig. 3.4. Simulink subsystem representing $\dot{z} = -\gamma|\dot{x} - \dot{y}|z|z|^{n-1} - \mu(\dot{x} - \dot{y})|z|^n + A(\dot{x} - \dot{y})$

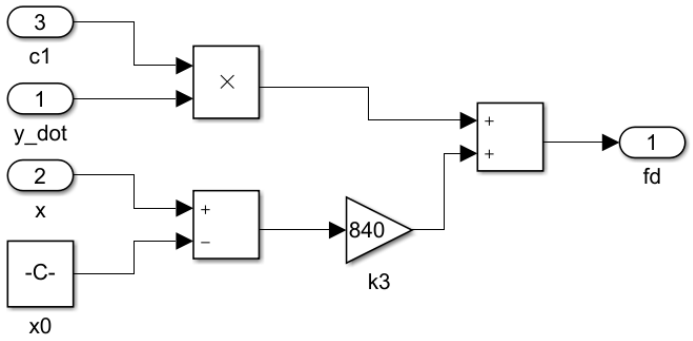

Fig. 3.5. Simulink subsystem representing $f_d = c_1\dot{y} + k_3(x - x_0)$

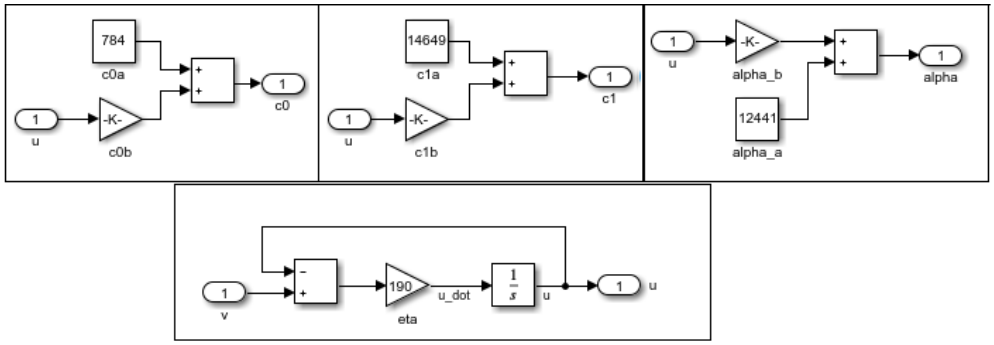

Fig. 3.6. Simulink subsystem representing equations for $c_0, c_1, \alpha \; and \; u$

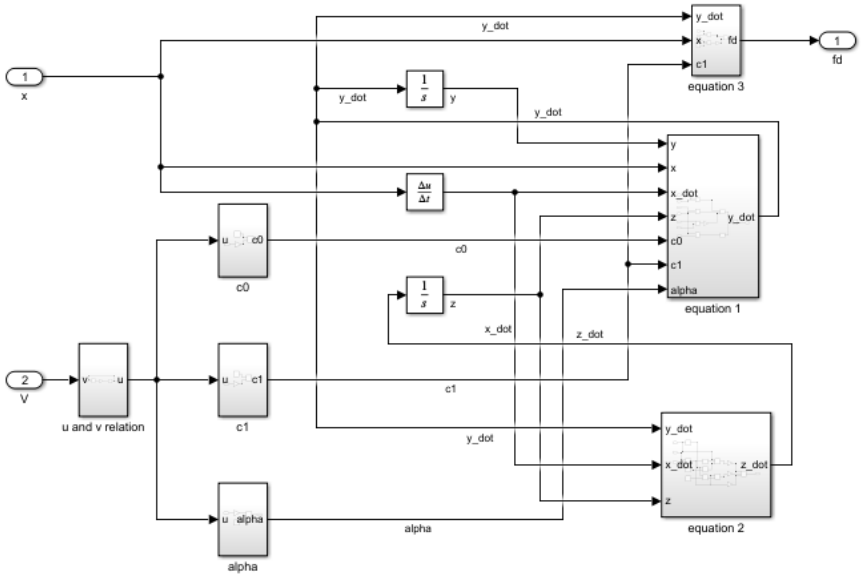

Fig.3.7. Simulink model of complete modified bouc wen model (connecting all above equations)

The parameters used for the model are obtained from literature as follows:

Table 3.1. Parameter values used in MR Damper simulation

Parameters	Values	Unit
c_{0a}	784	Ns/m
c_{0b}	1803	Ns/mV
k_0	3610	N/m
c_{1a}	14649	Ns/m
x_0	0.0245	m
η	190	s^{-1}
α_a	12441	N/m
α_b	38430	N/mV
γ	13632	m^{-2}
μ	2059020	m^{-2}
A	58	-
k_3	840	N/m
N	2	-

Results of MR Damper Simulink simulation.

Force Displacement and Force Velocity graphs were plotted from the above model as shown in Fig 3.8. The force output of the MR Damper was similar to a square wave. This shows its non-linear properties.

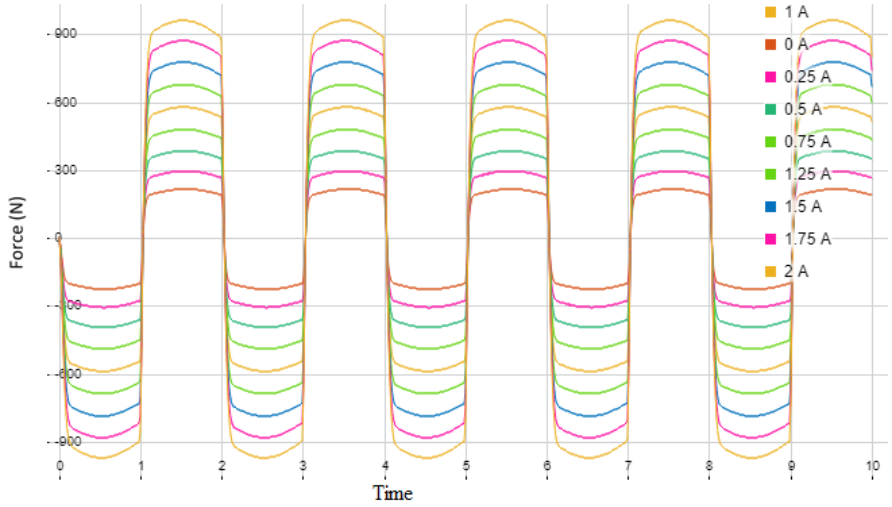

Fig 3.8: Force output for MR Damper with sinusoidal displacement input

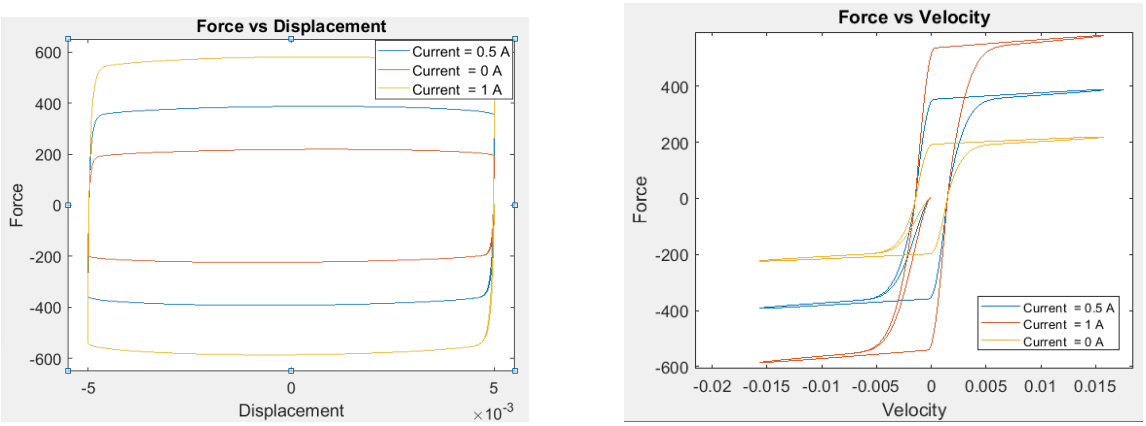

Fig 3.9: Force Displacement and Force Velocity graphs

This was found to be consistent with similar studies from literature [30]. Thus the MR Fluid Damper model was successfully simulated using Simulink.

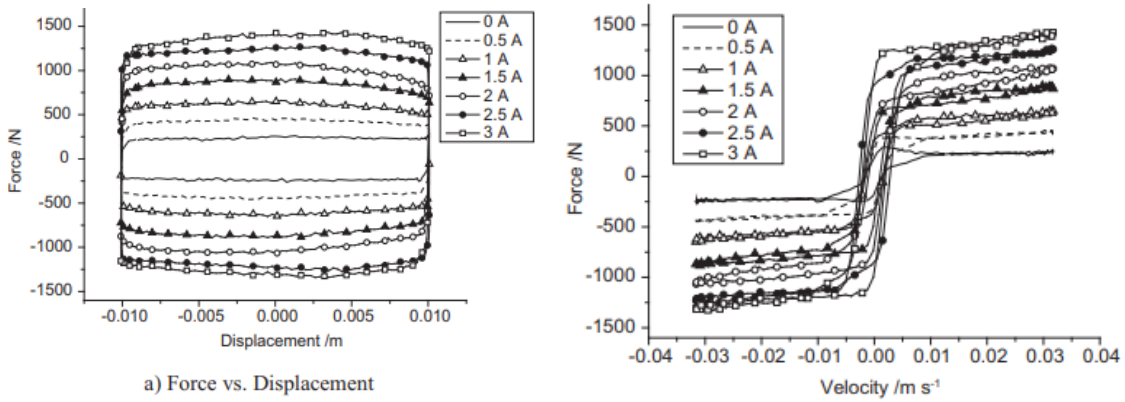

Fig 3.10: Force Displacement and Force Velocity graphs from literature

3.2.2 Adding MR Damper to Dynamic vibration Absorber model

The mathematical model of a vibrating system with a Dynamic Vibration Absorber is modelled as per equations 3 and 4. The MR Damper is added as Subsystem 3 (highlighted in Fig 3.11), which takes $(x2 - x1)$ as input x and gives f_d as output.

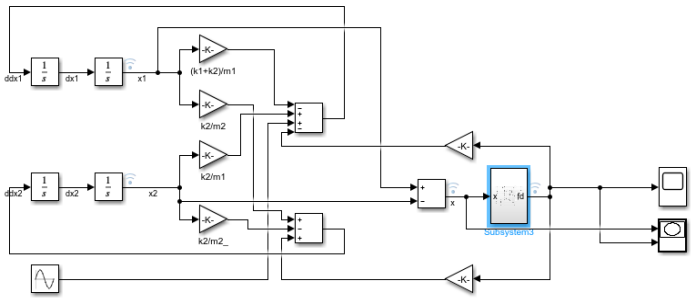

Fig. 3.11. DVA model with MR Damper subsystem highlighted.

The parameter used in the DVA is listed below.

Table 3.2: Parameter values given to the model

Parameters	Values	Description
m_1	44 kg	Primary Mass
m_2	5.5 kg	Absorber Mass (Secondary Mass)
k_1	55666 N/m	Supporting Stiffness
k_2	21012 N/m	Absorber Stiffness
m	0.244 kg	Rotating unbalance causing excitation
e	0.05 m	Radial eccentricity
ω	47.499 rad/s	Frequency of excitation

Results of MR Damper Simulink simulation.

The Bode plot was created on Matlab using the Bouc-Wen Model and it was found that the MRDVA model is successful in attenuating the vibration of the primary mass at resonance (when placed without the MRDVA system).

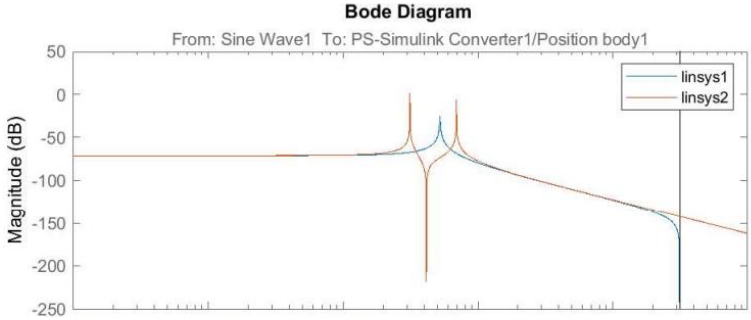

Fig 3.12 Output graphs from Simulink model of MR Damper DVA

3.2.3 MR Damper model – Bingham Model

Additionally, a Simulink model was also created for the MR damper using the Bingham Plastic Model

The Simulink model for the same is as shown below in Fig 3.12. This model is later use to fit data obtained from experimentation.

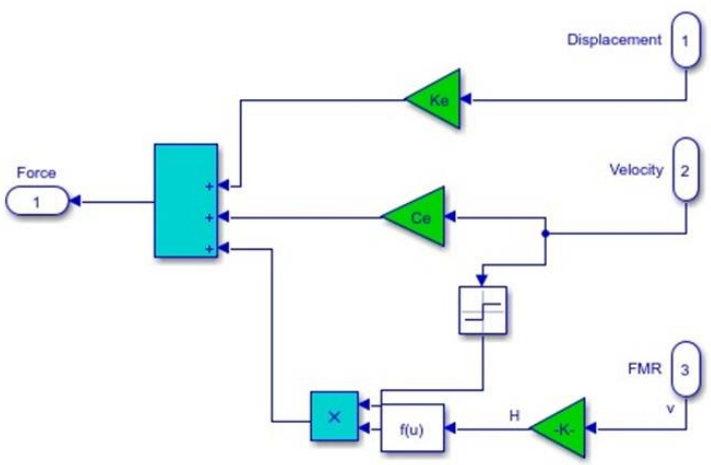

Fig 3.13 MR damper model created using Bingham plastic Model

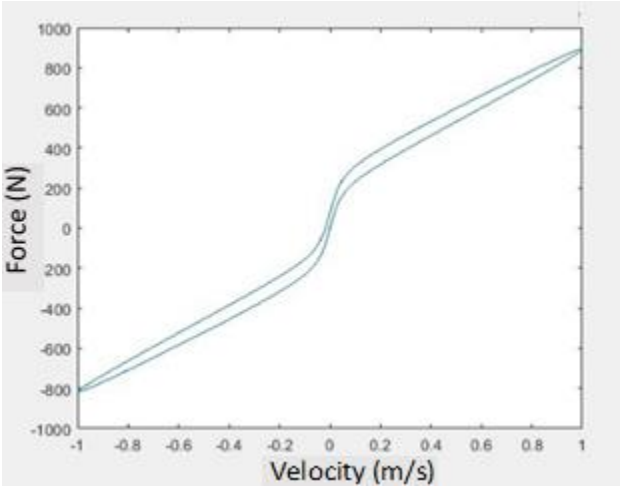

Fig 3.14 Force Velocity graph for Bingham model

CHAPTER 4
FINITE ELEMENT ANALYSIS OF MR DAMPER

4.1 MODELLING USING COMSOL

COMSOL Multiphysics is a FEM simulation software that can be used to conduct simulations with multiple physics modules. Since MR damper is a Multiphysics problem (Fluid and Magnetic Fields), COMSOL software was chosen to conduct simulations. For the purpose of simulation, the MR fluid had to be defined with input graphs and properties.

4.2 GENERAL DESIGN AND MODELLING OF DAMPER

To understand the behavior of MR Fluids in a damper with varying magnetic field, a simple geometry was created to represent the setup. An axisymmetric 2D model was created as this could easily represent all the features required. The specifications are as given below.

Table 4.1. Design Specifications of MR Damper

Parameter	Value
Damper Height	0.3 m
Damper Radius	0.05 m
Height of Piston	0.06 m
Radius of Outer End of Piston	0.02 m
Radius of Hole in Piston	0.005 m

The model consists of a damper, piston with a coil. The piston, named 1 and 2 in Fig 4.1, consists of a coil (named 2 in Fig 4.1.) and a core (named 1 in Fig 4.1.). Copper was assigned as the material for the coil and the core.

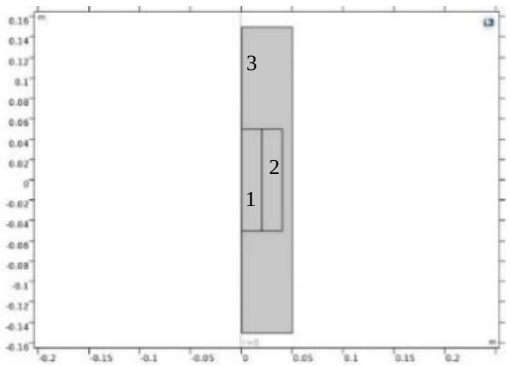

Fig 4.1. Model of Damper in COMSOL

4.3 MODELLING OF MR FLUID

A suitable MR Fluid for the application has to be chosen before simulation. The alternatives considered for this decision was MRF 140-CG, MRF 132DG, MRF 122EG, MRF 126LF and MRF 140BC.

MRF140BC were not recommended for Damper applications and so, was ruled out. MRF126LF was ruled out as it had lower settling resistance, which is an important property required for the damper application in the long run. Among the other options, the fluid which can achieve larger yield stress values at lower power was chosen, which was MRF 140CG. It also has high plastic viscosity when no current is applied, allowing it to still possess good damping properties.

The MR fluid will be assigned to part 3 of the model shown in Fig 4.1. The values for the parameters of LORD MRF 140CG were obtained from its datasheet and the required ones are tabulated below.

Table 4.2. Datasheet for LORD MRF 140-CG

Parameter	Value
Density	3540 kg/m^3
Relative Permittivity	5
Electric Conductivity	0.00000002 S/m

As MR Fluid does not show a constant permeability, its B-H Curve was utilized as obtained from the datasheet. The data was provided as an interpolation function in COMSOL.

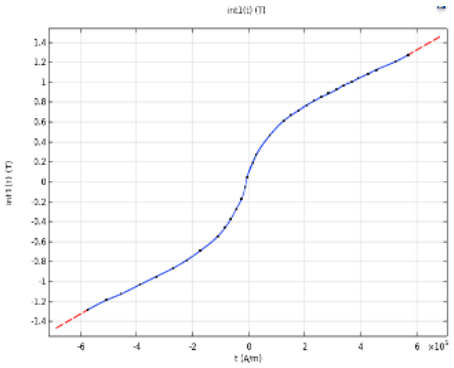

Fig 4.2. B-H Curve interpolated in COMSOL

4.4 FLUID PROPERTIES

The most important property of MR Fluid is the variation of rheological properties with magnetic field. To model this, two different approaches were adopted.

4.4.1 Variation of dynamic viscosity with magnetic field.

A simple Laminar flow was chosen as the physics model. Dynamic viscosity vs. Magnetic Flux Density graph was put forward in paper by A. Roszkowski, M. Bogdan, W. Skoczynski, and B. Marek [31]. This graph was used to specify the dynamic viscosity of the MR Fluid with respect to Magnetic Flux Density. The graph as a COMSOL interpolation function is given below.

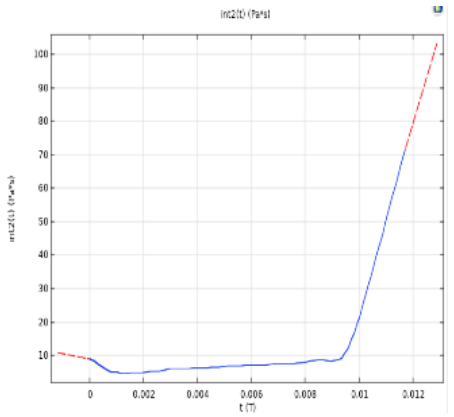

Fig. 4.3. Dynamic viscosity vs. B plot for MRF 140-CG as an interpolation function in COMSOL

4.4.2 Bingham-Papanastasiou Model.

In the second method, COMSOL's built-in non-Newtonian fluid model was used. Inelastic non-Newtonian constitutive relation was chosen under fluid properties of the Laminar flow study. Further, the Bingham-Papanastasiou inelastic model was chosen to represent the MR Fluid. This model is proven to be able to closely approximate the ideal discontinuous model of MR Fluids and describe fluid features accurately without adding unnecessary complications [32].

Here, viscoplastic fluid behaviour is characterized using yield stress, which is readily available to us from the LORD MRF 140-CG datasheet as a function of magnetic flux density. The constitutive relation is as follows:

$$\mu_{app} = \mu_p + \frac{\tau_y}{\dot{\gamma}}, |K| > \tau_y$$

Where

$$\mu_{app} = apparent\ viscosity$$

$$\mu_p = plastic\ viscosity$$

$$\tau_y = yield\ stress$$

$$\dot{\gamma} = Shear\ rate$$

Regularization of viscosity in the yielded and unyielded region is achieved by the following relation,

$$\mu_{app} = \mu_p + \frac{\tau_y}{\dot{\gamma}}[1 - e^{-m_p\dot{\gamma}}]$$

Where m_p controls the exponential growth of stress. [32]

Here,

$$\mu_p = 0.28\ Pa.s$$

$$m_p = 0.25\ s$$

τ_y is given from the yield stress vs magnetic field intensity graph as shown in Fig 4.4.

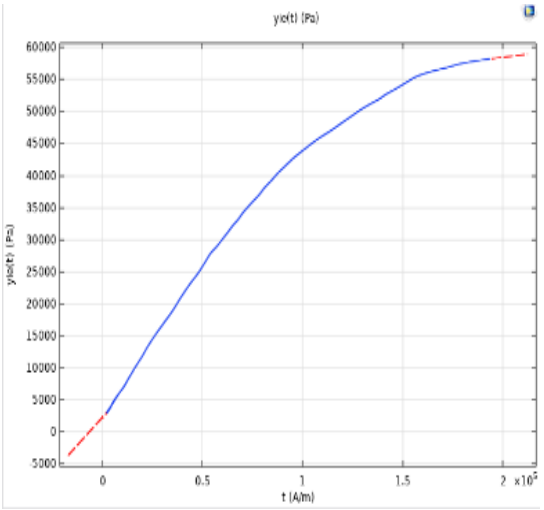

Fig 4.4. Yield Stress vs Magnetic Field Intensity Plot for MRF 140-CG plotted in COMSOL

The Bingham-Papanastasiou model was chosen for further analysis. MR Fluid shows non-Newtonian characteristics in the presence of a magnetic field, and this is taken into account by the Inelastic non-Newtonian constitutive relations in COMSOL. The velocity profiles obtained through both methods are shown below for reference. A faster change in velocity is observed in the Bingham-Papanastasiou model.

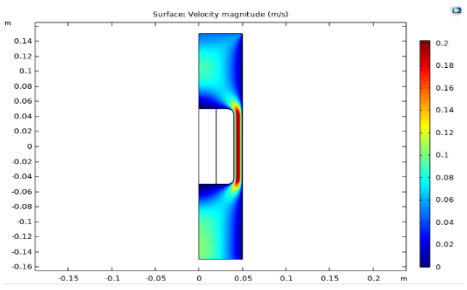

(a)

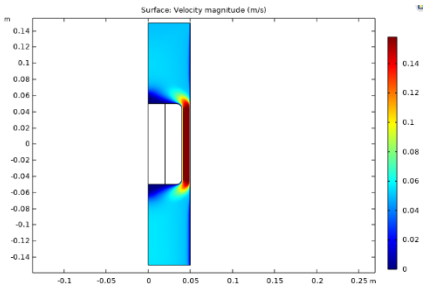

(b)

Fig 4.5. (a*)* Dynamic Viscosity with Magnetic field Model (b) Bingham-Papanastasiou Model

4.5 METHOD OF STUDY AND PHYSICS USED

To obtain the required results, two physics models were required in COMSOL, magnetic fields (m_f) and a flow physics. For this model, laminar flow physics (spf3) was chosen, and the above mention non-Newtonian properties were introduced.

A Grid Independence test was conducted to get an optimized mesh setting. A free triangular mesh was utilized for the same. The results are as shown below in Fig 4.6. As the mesh size decreases (towards left), the variation in output is observed to be negligible. The built-in extra fine mesh setting with maximum element size 0.00065 mm was used for the study.

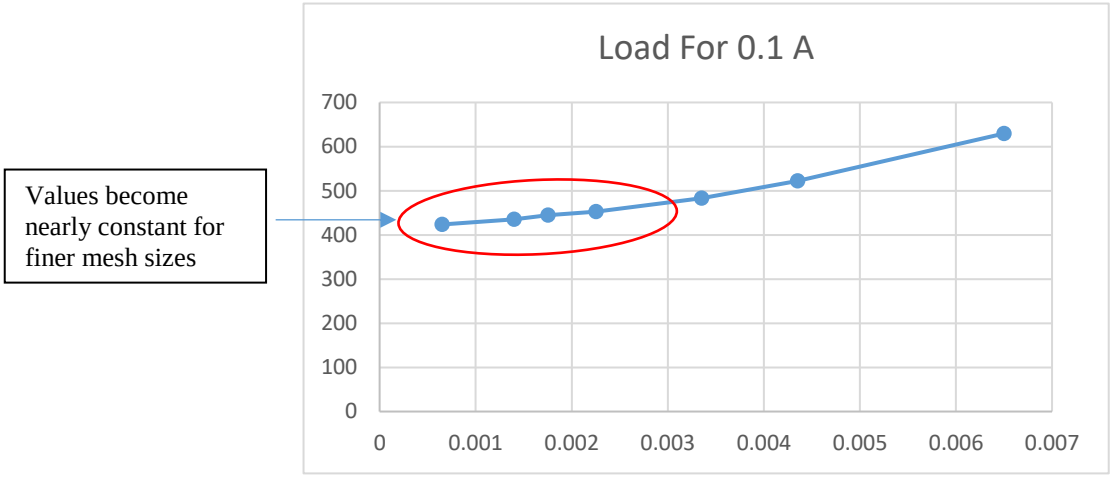

Fig 4.6 Graph of grid independence test

Magnetic Analysis

For the magnetic study, magnetic properties of the iron core were obtained from the built-in model, while MR Fluid data was given from the dataset (Table 4.3).

Table 4.3: Initial and Boundary conditions given to the Magnetic Analysis module

Initial conditions	**For t = 0**	**For all x, y**		**Magnetic vector potential = 0Wb/m**
Boundary Conditions	t > 0	x = 0	Axial Symmetry	
		x = 5 cm, y = 15 cm, y = -15 cm (Damper walls)	Magnetic insulation	

Region 2 (Fig 4.1) was assigned as a homogenized multiturn coil, with 700 turns and 0.1 A as the excitation current. The coil wire parameters were set as default, i.e., Wire conductivity = $6 \times 10^7 \frac{S}{m}$ and wire cross-sectional area =$1 \times 10^{-6}\ m^2$.

Fluid Flow Study

The aim is to simulate a simplified model of MR Fluid flowing over the region of influence of a magnetic coil in the piston. So, a stationary model was chosen. The uppermost boundary is chosen as an inlet with Fluid velocity of 5 cm/s. The lower boundary is an outlet with gauge pressure zero.

Table 4.4 : Initial and Boundary conditions given to the Magnetic Analysis module

Initial conditions	**For t = 0**	**x ≥ 0, y ≥ 0**		**Velocity field (u_r, u_z) = 0 m/s Pressure (P) = 0 Pa**
Boundary Conditions	For t > 0	x = 0	Axial Symmetry	
		x = 5 cm (Damper outer walls) & (Piston outer walls)	Wall boundary condition	
		y = 15 cm	Inlet	Velocity u_y = -0.05 m/s
		y = -15 cm	Outlet	Pressure P = 101325 Pa

Fluid Structure Integration

An important result to be obtained from the model was the stresses and force on the piston. This will translate as the damping force in the damper. In order to obtain this, a Fluid-Structure interaction Multiphysics study was also introduced. This simulates the piston as an elastic body and obtains the forces and stresses on it.

4.6 RESULTS FROM COMSOL MODEL

Before the simulation of the above model, a simpler model of fluid flow in a straight pipe was simulated. MR Fluid (with properties as given in Section 2.2) was modelled to flow down a long pipe with magnetic field applied only at section 2 (as shown in Fig 4.1). A uniform flow was observed in section 2 due to the higher viscosity. This shows that magnetic field changes the rheological properties of the fluid and thus can help control damping properties.

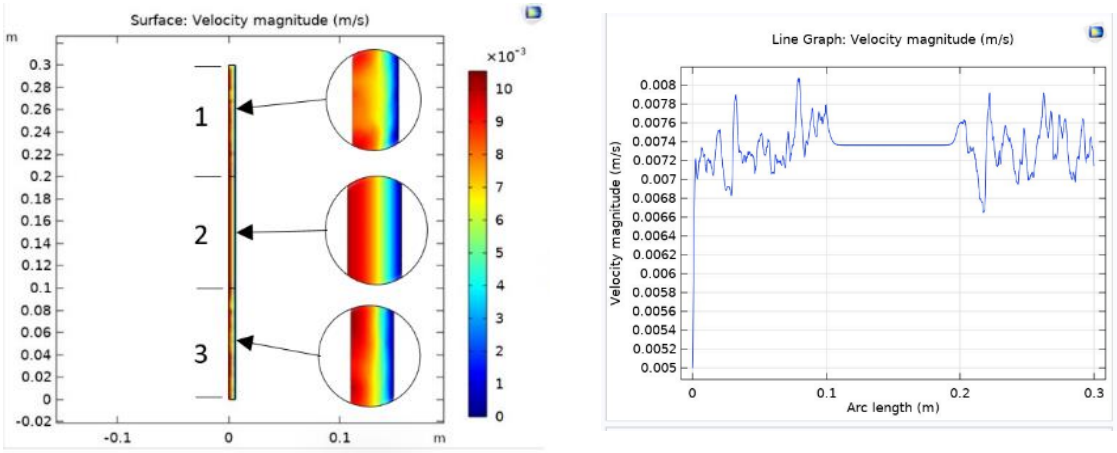

Fig 4.7. Variation of velocity in the presence of a magnetic field

The results obtained from the model described in the previous sections is discussed in the following sections.

Magnetic Analysis

Fig 4.8 shows a plot of Magnetic Flux density (B) and Field intensity (H) in the damper model. The high H value in the annular gap gives higher resistance to the flow in this region. This allows us to control the damping force and associated properties.

A plot of the Magnetic flux density shows the sudden drop of B in the MR Fluid region. As shown in Fig 4.8, the maximum value is in the range of 10^{-10}. This might affect MR Fluid's controllability and might call for an improvement in coil design and selection of MR Fluids.

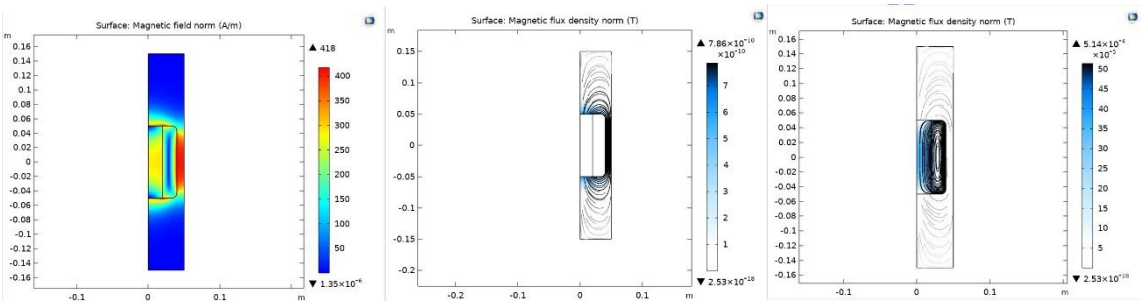

Fig. 4.8. (a) Magnetic Flux Density (B) (b) Magnetic Field Intensity (H)

Fluid Flow Analysis

The Bingham Papanastasiou model was chosen to continue the study. The velocity field is shown. As expected, high velocity is observed at the narrow region of flow. The maximum velocity is 0.2 m/s, and the minimum velocity close to zero is observed at the middle of the piston. Boundary layer is observed to be very thin.

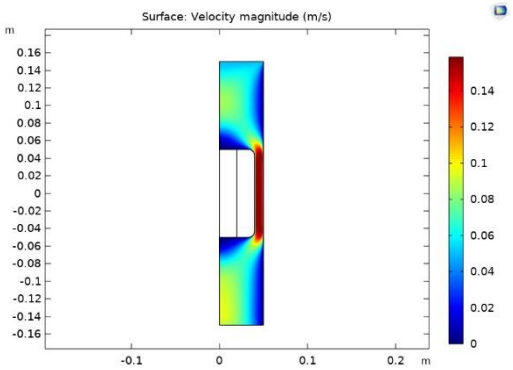

Fig 4.9. Velocity of Flow

Force Analysis

The effectiveness of a damper is obtained from the force applied on the piston. The load magnitude on the piston surface is plotted as a line plot to understand the load and its variation. The highest value of load magnitude is 1.56 x 10^4 N/m^2.

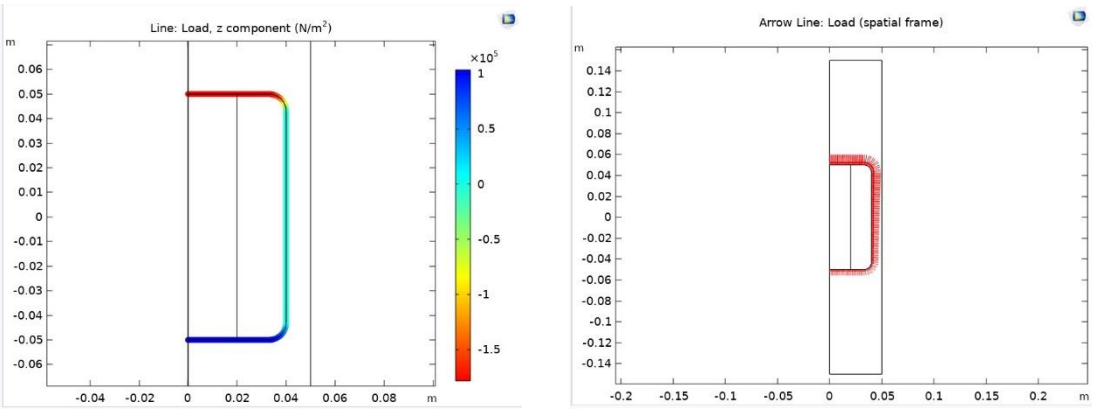

Fig 4.10. (a) Velocity of Flow. Force on Piston (b) Arrow line diagram (c) Line load diagram

The total force was calculated as the integral of the z component of the load on the fluid-solid boundary. This was calculated for different values of current passing through the coil to understand the variation. As observed from Table 4.5, the load increases with an increase in current.

Table 4.5. Variation of Load in Component with Current in Coil

Current in the coil (A)	Load - z component (N)	Velocity (m/s)	Highest Magnetic Flux density (T)
0	-405.61	0.15	0
0.05	-414.78	0.15	2.57 × 10−4
0.1	-423.65	0.15	5.14 × 10−4

CHAPTER 5

CAD MODELLING

5.1 MR DAMPER

An MR Damper was initially modelled by taking the dimensions from a standard MR Damper. The original prototype was then further improved with design modifications to suit application in a MR DVA system and with innovations to improve performance.

A twin tube MR damper was modelled using SolidWorks.

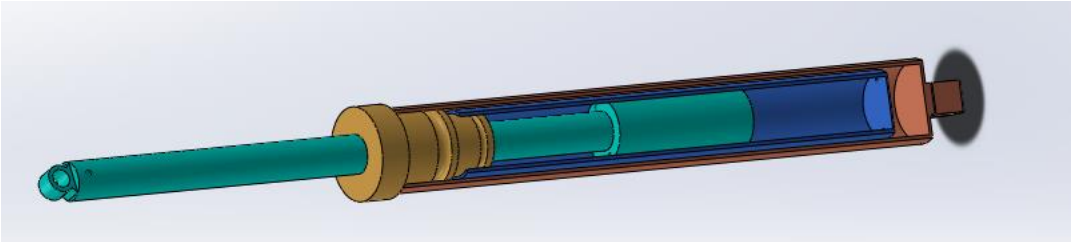

Fig 5.1 : Assembly of twin tube MR Damper

After modelling the standard MR damper another Damper in which the length is reduced was designed. The Length of the damper was reduced because for the purpose of using it in a DVA, the Damper is only going to work with Vibrations that are low displacement disturbances as opposed to the high amplitude disturbances that standard MR Dampers are designed for.

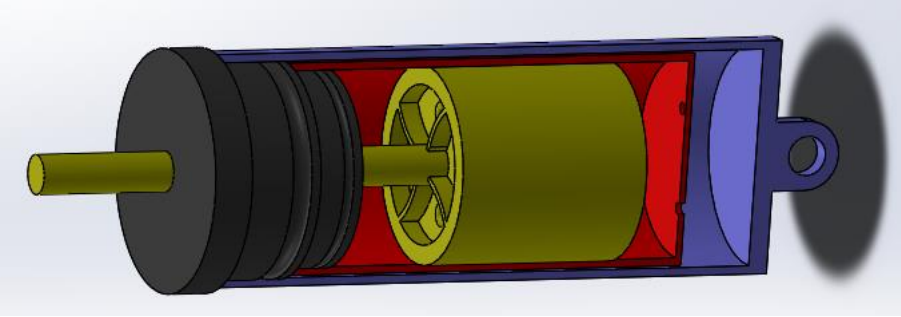

Fig 5.2: Solidworks model of the MR damper with agitator piston and reduced length

5.2 DAMPER TESTING SETUP

A simple experimental setup as seen in Fig 5.3 has been modelled in CAD software. This setup utilizes a motor to provide the required actuation for the damper.

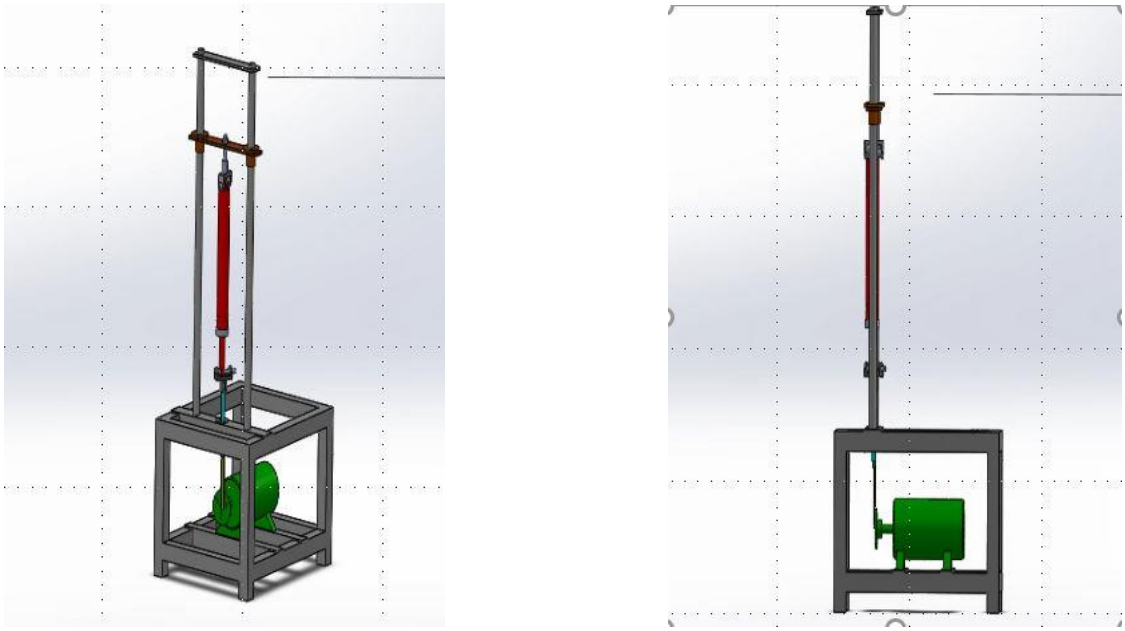

Fig 5.3 : Isometric view and Side view of the experimental set up

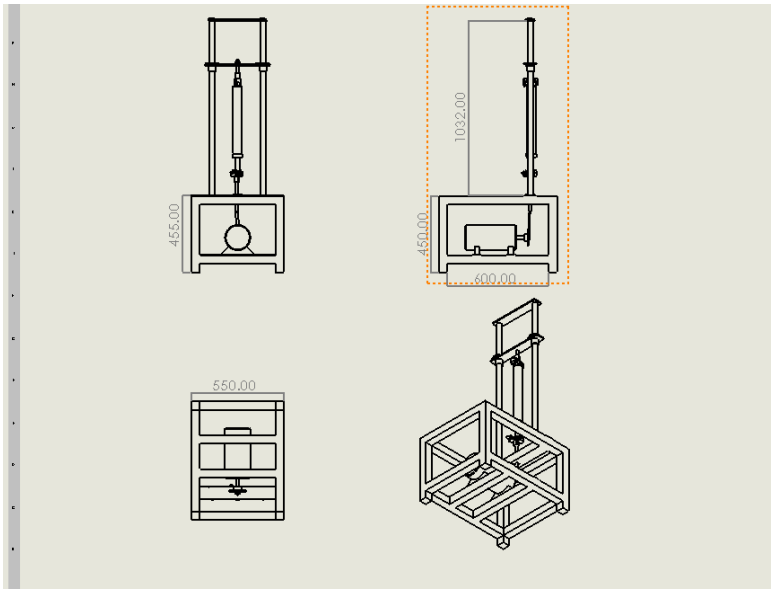

Fig. **5.4** 2D drawings of the experimental set-up in SolidWorks

5.3 DVA TESTING SET UP

For the experimentation of the DVA a setup was designed. The setup requires a motor as prime mover. A sinusoidal output is required, which maybe be obtained from a simple mechanism. This output is then transferred to the base and then to the primary mass. The primary mass holds the MRDVA consisting of springs and MR damper. Multiple iterations of the setup were designed using SolidWorks as seen in below.

5.3.1 Selection of input

In order to conduct experiments on DVA, a sinusoidal input is preferred. Many options were considered to convert the output of the motor to a linear sinusoidal motion. One of these options was a scotch yoke mechanism (Fig 5.5), in which there is a disc (or slotted holder) with a rod protruding out of it with an eccentricity. This rod is then placed in a slot which transfers the motion in s single degree of freedom. This method could provide several amplitudes of vibration and a perfectly sinusoidal input.

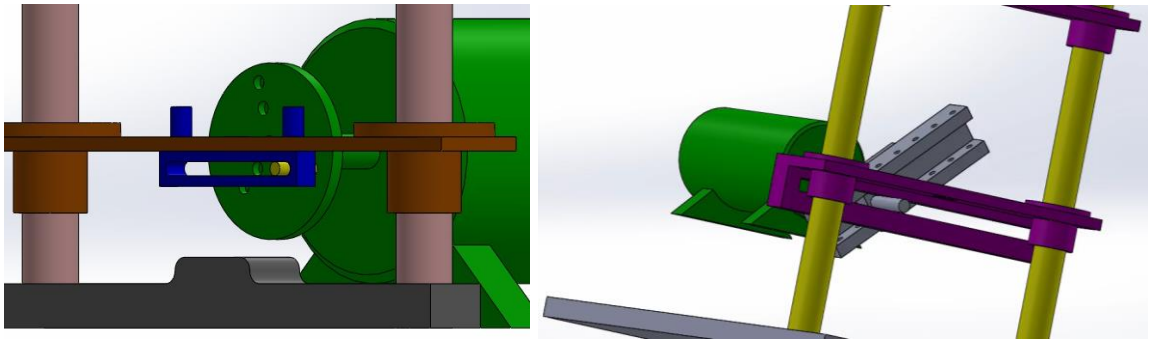

Fig 5.5 Two iterations of scotch yoke mechanism

Though providing a perfectly sinusoidal input, this method would be more difficult to fabricate as it requires strong pins and holders of very small size.

The second method was to use a cam follower mechanism. Different types of cams would provide different nature of inputs. Considering that the MR DVA would be working with vibrations that tend to have smaller amplitudes, cams having small eccentricities would suffice. Also cam-follower mechanisms are readily available and can be used as the vibration provider.

Options with cam follower setup were also considered as shown in Fig 5.6.

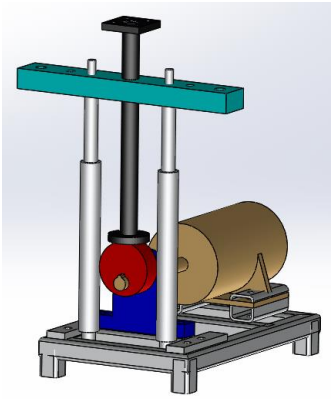

Fig 5.6 Base excitation system

5.3.2 Design of DVA system

A two degree of freedom model is designed in which the masses are allowed to slide on two rods connected to a fixed base. The damper is placed connecting the primary and secondary masses. A cap is provided on the top of the system to provide additional stability and prevent twisting of the rods. A base sliding plate is connected to the follower rod. Springs are placed along the rods between the base plate and primary mass and the secondary mass. The secondary system without the vibration provider was initially designed as seen in Fig 5.7. Then this system was combined with the designed cam follower setup to create the complete DVA testing setup.

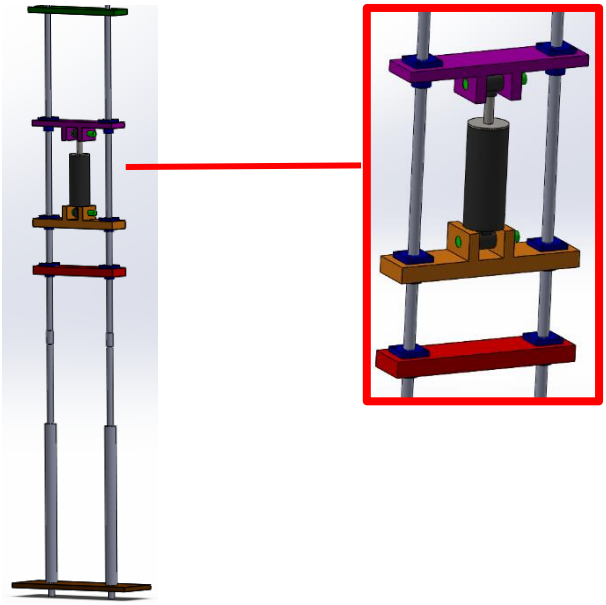

Fig 5.7 Arrangement of the masses on the rods with the MR Damper in position

The final model was developed after combining both the designed parts as shown below in Fig 5.8.

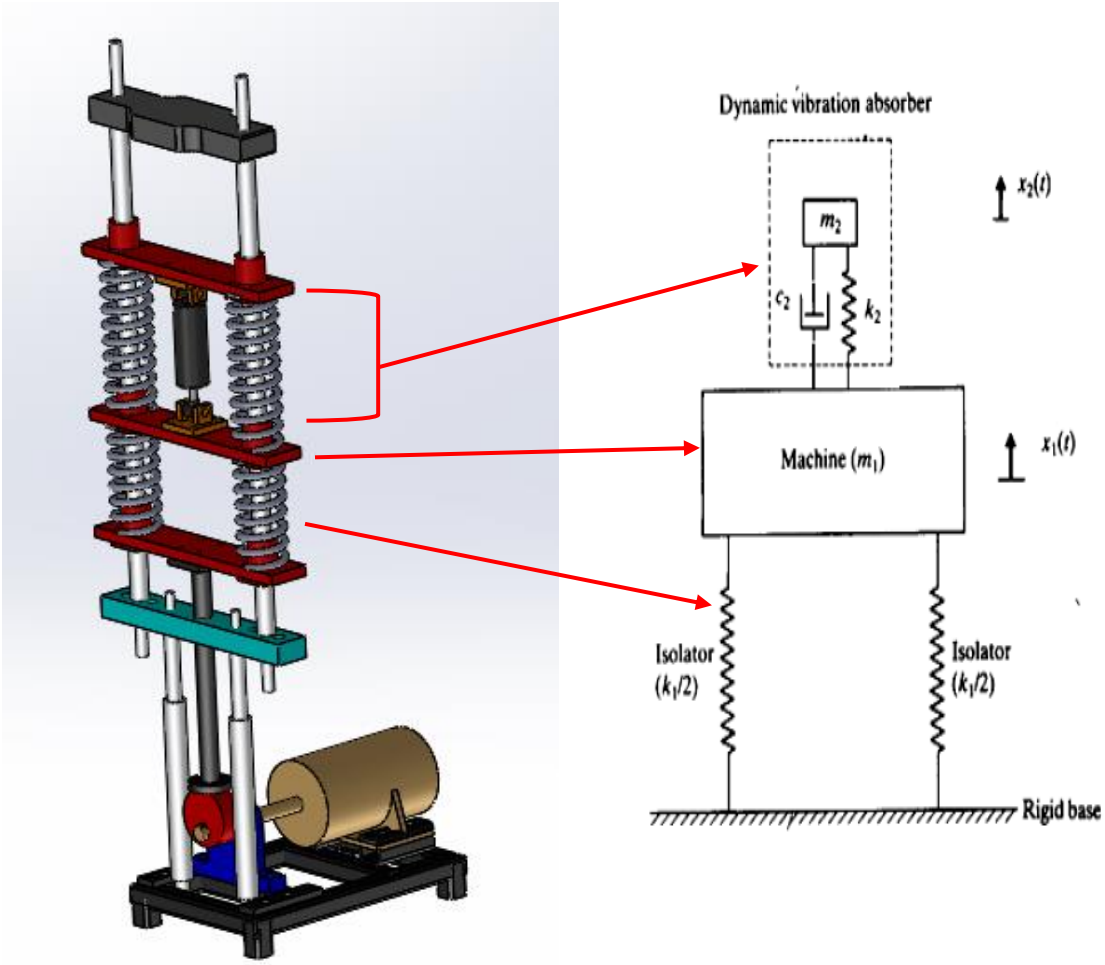

Fig 5.8 Final cad model for experimental setup compared with initial schematic

CHAPTER 6

FABRICATION OF SET UP

6.1 PRELIMINARY DESIGN OF SETUP

The basic requirement for design of experimental setup was that it should be a fair representation of a vibration system whose natural frequency is in a range that can be conveniently experimented and tested. As the available motor had a maximum speed of 1500 rpm, the system should have a natural frequency around 500 rpm to be able to test conveniently around this speed.

Also considering the space and material availability in the laboratory, masses ranging from 1 to 5 kg could be procured for representing primary mass and secondary mass. Thus, two primary masses were decided on: 4kg and 1.3kg.

The spring required was calculated such that the highest natural frequency (i.e., for 1.3 kg) will be at 500 rpm.

Natural frequency = 500 rpm = 52.35 rad/s = 8.33 Hz

So $k = \omega^2 m = 52.35^2 x 1.3 = 3562.68 \frac{N}{m} = 3.562 \frac{N}{mm}$

As 2 springs will be used in parallel,

K of one spring = 3.562/2 = 1.781 N/mm

Same spring was used for 4 kg as well.

The natural frequency of that system is calculated

$$\omega = \sqrt{\frac{k}{m}} = \sqrt{\frac{1781 \times 2}{4}} = 29.841 \frac{rad}{s} = 4.75\ Hz = 284.96\ rpm$$

The secondary masses were selected based on required conditions.

1. Secondary system is designed such that there is minimum oscillation at the natural frequency of the primary system. Thus,

$$\sqrt{\frac{k2}{m2}} = \sqrt{\frac{k1}{m1}}$$

Thus, for the 1.3 kg mass, m2 = 0.9 kg and k2 = 1.233 N/mm can be used as secondary system. For 4 kg, m2 = 1.3 kg and k2 = 1.233 N/mm can be used.

2. Secondary system is designed for maximum efficiency as a standalone vibration absorber.

   This is obtained when

$$\frac{\omega_1}{\omega_2} = \frac{1}{1 + \frac{m2}{m1}}$$

   So after calculations, we can see that $m_1 = 4\,kg$ and $m_2 = 0.9\,kg$ satisfy this condition.

6.2 MR DAMPER

An MR Damper needed to be procured to be a part of the system. The dimension of our proposed system along with the range of motion, mass etc. was considered and the MagneshoX mini–MR Damper was acquired. Since the system deals with vibrations a damper with the least stroke length was selected.

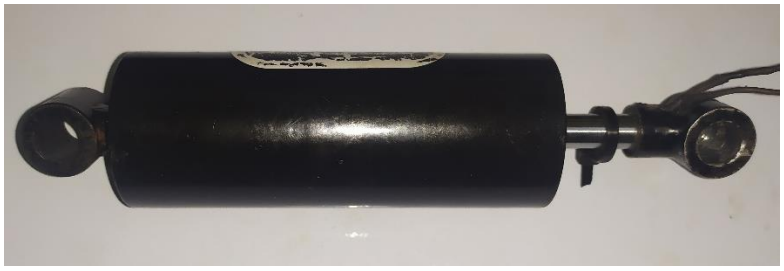

Fig 6.1. MagneshoX MR damper

6.3 MR DVA COMPONENTS

The base excitation setup consisting of a motor connected to a cam follower system was selected to provide input to the DVA system. The follower rod was connected to a base plate that transfers the vibration through a set of springs to the primary mass. The primary mass is then connected to the secondary system via a set of springs and the damper. Finally, a cap is provided to establish further stability.

6.3.1 Selection of Bearings

In order to let the masses, slide along the rods, linear bearings will be provided. The inner diameter of the linear bearing needs to match the diameter of the sliding rods. For this purpose, LMK bearings were selected.

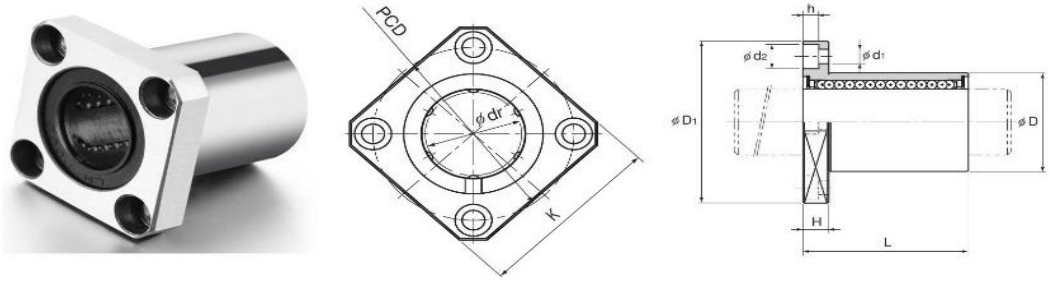

Fig 6.2. Diagram of linear bearing used for setup

6.3.2 Selection of Springs

Before acquiring the springs, certain calculations needed to be performed to prevent buckling and ensure appropriate stiffness. Two inner diameters were selected for two sets of springs, one to perfectly fit the 21 mm rod on which the bearing is going to placed and the other to fit the flange end of the LMK bearing that was chosen. The calculations were done considering 4 mm wire made of oil hardened spring steel wire. A sample calculation is given below

Requirements:

1) Inner diameter = 36 mm (Considering compatibility with bearings)
2) Natural frequency = 500 rpm = 52.35 rad/s = 8.33 Hz

So $k = \omega^2 m = 52.35^2 x 1.3 = 3562.68 \frac{N}{m} = 3.562 \frac{N}{mm}$

K of one spring = 3.562/2 = 1.781

3) Free length = 150 mm

Consider 3 mm wire, made of oil hardened and tempered spring steel wire.

Modulus of elasticity = 205 880 MPa

Modulus of rigidity = 81370 MPa

$Spring\ index(C) = \frac{D_m}{D_w} = \frac{39}{3} = 13$ (C should be between 5 and 12)

We know K, so we can find the number of active coils:

$$No.of\ active\ turns(Na) = \frac{Gd^4}{8D^3k} = \frac{81370x3^4}{8x39^3x1.781} = 7.8 = 8\ \text{turns}$$

Free length given as 150 mm

$$Critical\ ratio = \frac{62}{150} = 0.4133$$

$$\frac{L_f}{D_m} = \frac{150}{39} = 3.85$$

This comes in the stable region

$$Lenght\ of\ spring(L_f) = N \times P + 2 \times D_w$$

$$Pitch\ (P) = (L_f - 2 \times D_w)/N = (150 - 2 \times 3)/8 = 18\ mm$$

$$Solid\ length\ = D_w \times (N_a + 2) = 3 \times (10) = 30\ mm$$

$$Compressible\ length = 150 - 30 = 120\ mm$$

These calculations were repeated for the different spring conditions. This was done so that different combinations of springs can be tested. The table containing all the calculated values is given below.

Table 6.1 Specifications of springs used for experimentation

	K (N/mm)	**Free Length (mm)**	**Number of active coils**	**Inner dia (mm)**	**Outer dia (mm)**
Spring1(1)	3.562	150	15	22	28
Spring1 (2)	1.781	150	30	22	28
Spring1(3)	1.781	150	8	36	42
Spring2(1)	1.233	194	30	36	44
Spring2(2)	1.233	194	35	22	28
Spring2(3)	0.68	194	17	36	44

For proper fixing, squared and ground coils are used. The purchased springs were then tested in a UTM machine to verify their values. The UTM machine gave a stress vs strain graph as shown in Fig 6.3.

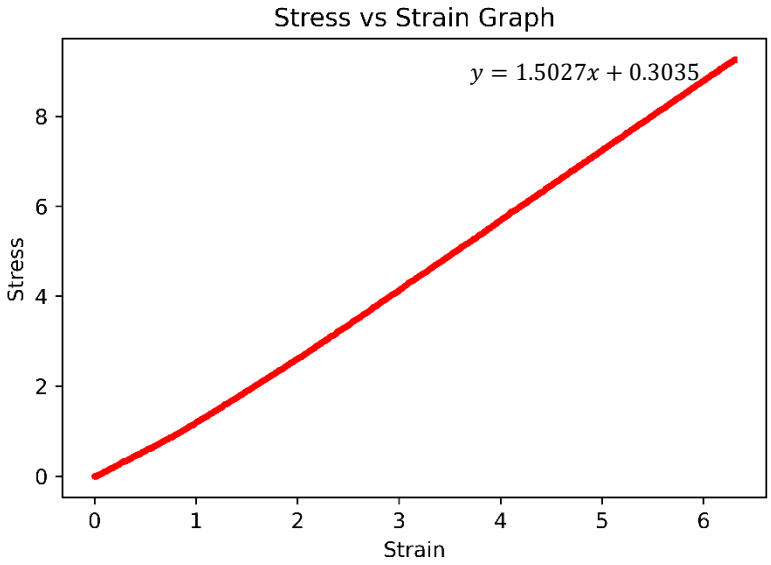

Fig 6.3. Graph showing stress vs strain curve obtained from UTM while testing spring

The slope of the stress vs strain graph gives the stiffness of the spring. In Table 6.2 the stiffness required and actual stiffness of the spring is given.

Table 6.2 Experimental vs calculated stiffness of springs

Spring name	**Stiffness obtained from UTM Experiment**	**Stiffness calculated during design**	**Remarks**
Spring 1 (2) a	1.6122	1.781	k_1
Spring 1 (2) b	1.6122	1.781	k_1
Spring 1 (3) a	1.3364	1.781	k_1
Spring 1 (3) b	1.5027	1.781	k_1
Spring 2 (1) a	2.5375	1.37	k_2
Spring 2 (1) b	2.5979	1.37	k_2
Spring 2 (2) a	1.8095	1.37	k_2
Spring 2 (2) b	1.7541	1.37	k_2

6.3.3 Spring Mounts

When operating the DVA at high speeds and resonance there is chance for the mass to be separated from the spring due to the inertia of the mass. Also, it is necessary to ensure that the springs stay aligned with the mass and don't slide to the side while operating the DVA. To solve these two issues a spring mount was designed. A plate is made from sheet metal and a depression is provided for the spring to rest in. This prevents the spring from misaligning with the masses. Holes are provided for the bolts that pass through the LMK bearings. The bolt heads will fasten the mass to the spring. This solves the issue of the mass being separated from the spring and ensures that the motion is transferred effectively and continuously. This mount is machined using CNC machine.

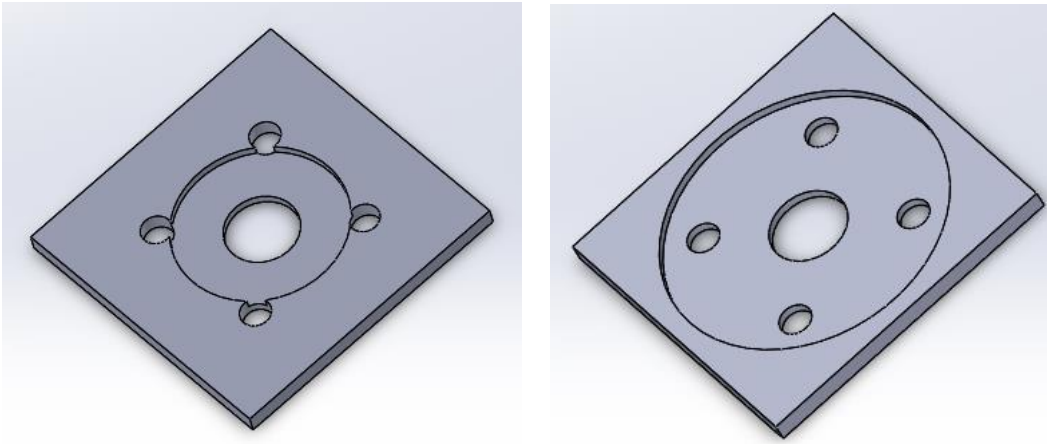

Fig 6.4 Spring mounts for the 28 (left) and 44 (right) diameter springs

Fig 6.5 Spring resting in mount with the bolts held in place

6.3.4 Fabrication of Masses

The masses were designed with holders for the damper and with two holes on either side for the LMK bearings. The Bearings will then be placed on the two rods and allowed to slide. FEM analysis was done on the masses to test the deflection under required load, as shown in Fig 6.7. The factor of safety was considered and the deflection was within limits. The masses required for the DVA were calculated so as to keep the natural frequency, ω as constant.

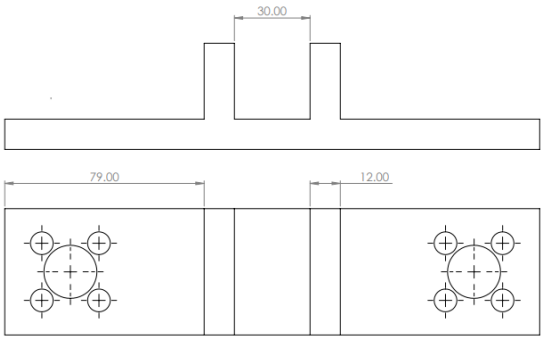

Fig 6.6 Drawing of mass

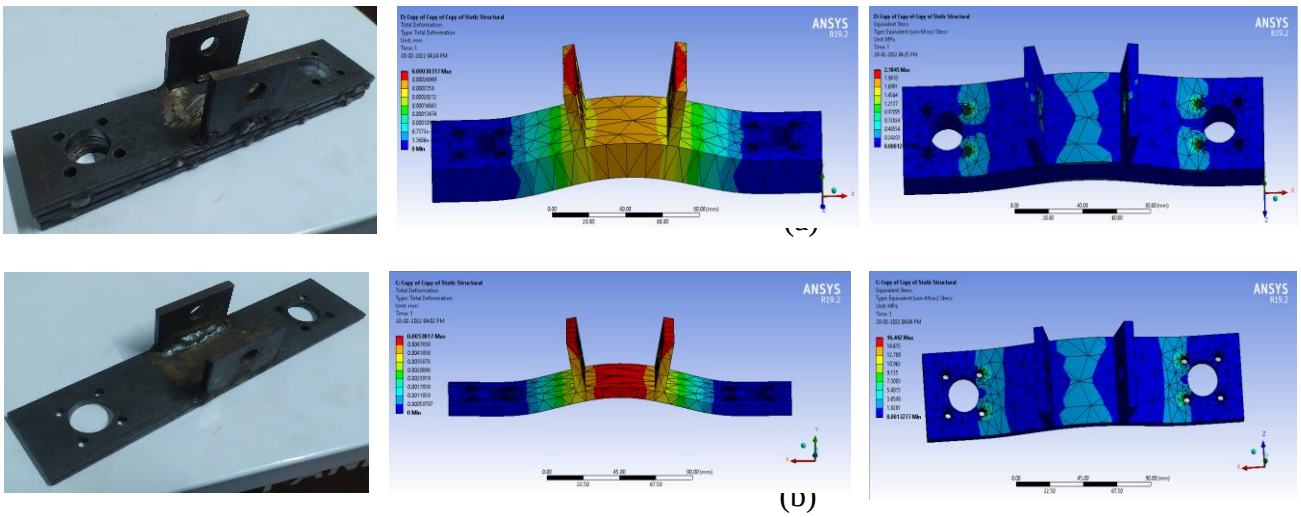

Fig 6.7 Mass and the FEM simulation of (a) primary mass and (b) secondary mass

Fig 6.8 4 kg mass

6.4 FINAL SETUP

According to the design obtained from calculations and simulations the final setup was fabricated and assembled. Many small design flaws and hurdles were overcome to obtain the final setup of MR Fluid based dynamic vibration absorber. Completely assembled setup as shown in Fig 6.9.

Fig 6.9 DVA testing setup (left) and control panel and motor used (right)

CHAPTER 7

EXPERIMENTATION

The setup was thus manufactured according to the simulations, calculations and design done prior. The working of this setup has to be verified using experimentation. This chapter talks about experiments conducted.

7.1 ADDITIONAL FACILITIES FOR EXPERIMENTATION

To simulate the required vibration a cam follower setup was obtained. This was attached to the base plate to provide sinusoidal oscillations. An eccentric cam and knife edge follower is chosen to obtain a sinusoidal profile for excitation.

The cam was run with a 0.5 hp motor. A VFD was also provided along with a control panel. This is used to control the frequency of the cam. There is a proximity sensor that measures the speed of the rotating shaft and thus provides rpm readings.

Measuring equipment used are mainly laser Sensors. This also required a DAQ for obtaining readings.

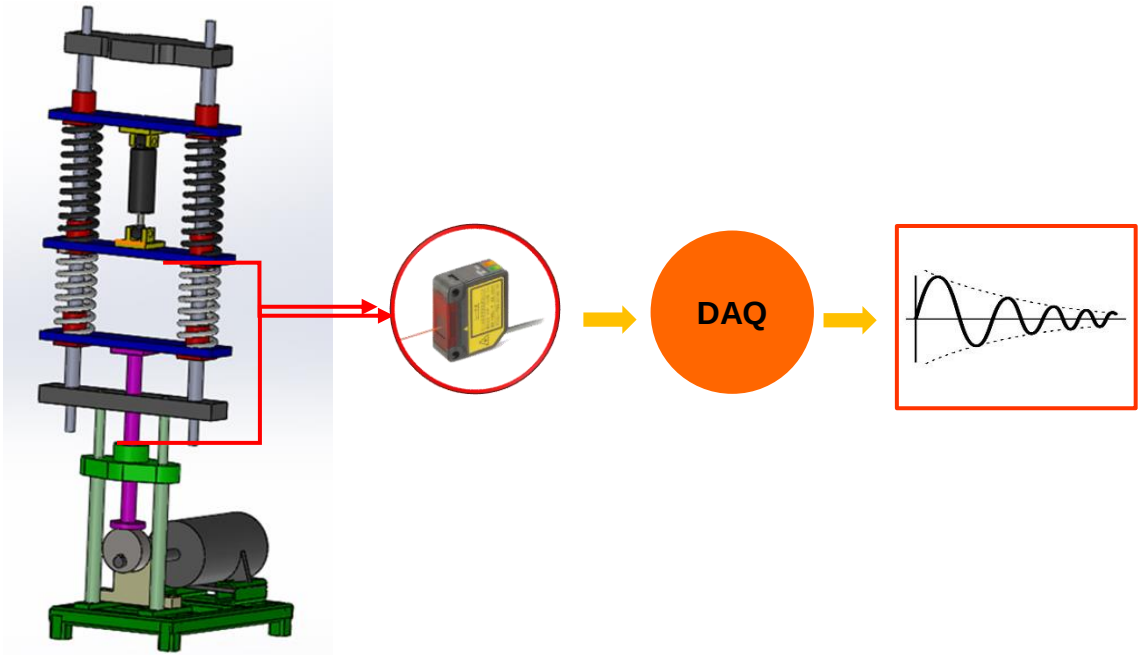

Fig 7.1 Experimental setup flow chart and signal flow chart

7.2 EXPERIMENTS CONDUCTED

7.2.1 Experiment No.1

Experiments on the damper setup was performed for two sets of masses as mentioned in design of experiments.

Set 1: m1 = 1.3 kg, m2 = 0.9 kg;

Set 2: m1 = 4 kg, m2 = 0.9 kg;

Objective

1. Confirmation of the natural frequency ω_P of the primary system.

Experimental Procedure: The SDOF system comprising of only the base plate and the primary mass will be subjected to harmonic base excitation with a fixed amplitude. The displacement of primary mass was then observed at different cam rotation speeds using the laser sensor. Data was captured for about 10 secs. The data generated plotted as Amplitude Ratio versus Frequency (Hz).

- Natural frequency calculated from the frequency at which maximum amplitude was achieved

7.2.2 Experiment No.2:

Objective

1. Check vibration reduction capability of passive DVA

Experimental Procedure: The 2-DOF system comprising of the base plate, primary mass and secondary mass will be subjected to harmonic base excitation with a fixed amplitude. The displacement of primary mass is then observed at different cam rotation speeds using the laser sensor. Data was captured for about 10 secs. The data generated plotted as Amplitude Ratio versus Frequency (Hz). The passive system is designed to provide vibration absorption at the natural frequency of the SDOF system. This is to be verified.

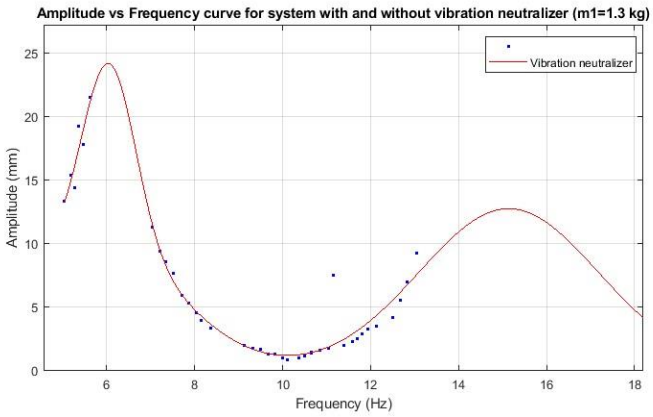

Fig 7.2 Experimental Frequency response plot for passive DVA system

7.2.3Experiment No.3:

Objective

1. Obtain MR Damper parameters to fit it into mathematical model

Experimental Procedure: The damper is subject to compression and tension. The F vs x and F vs v curves are plotted at different currents, with the help of a Load cell and accelerometer. This will help characterize the damper at different currents. This data can then be put into the mathematical model. The experimental setup with MR damper is shown in Fig 7.3.

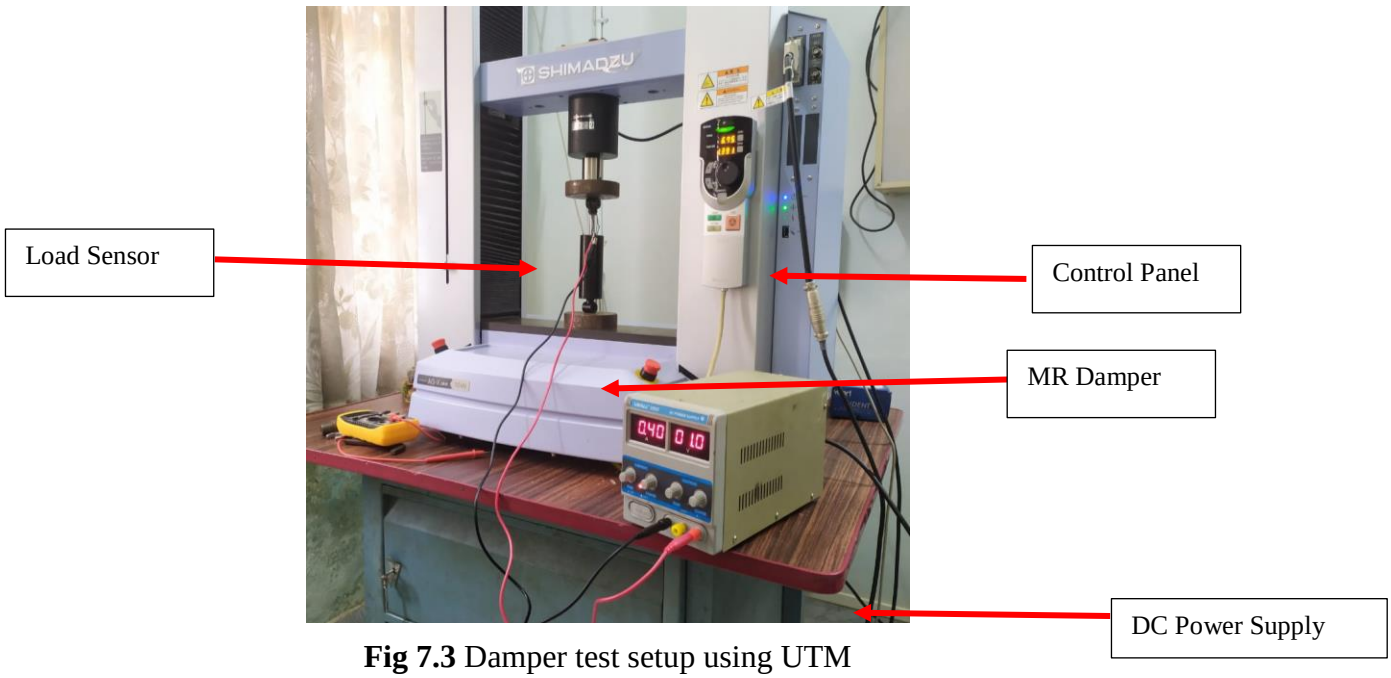

Fig 7.3 Damper test setup using UTM

7.2.4 Experiment No.4:

Objective: Find optimum damping at various input frequency

DEPENDANT VARIABLE:

1) Time taken to reach steady state
2) Final amplitude of primary mass vibration

FACTORS OR INDEPENDENT VARIABLES

1) Current provided to damper

Range: 0-2A

Levels: By changing the input current using Power Supply Unit

2) Amplitude and frequency of Input signal (Motor)

Range: 25 Hz (Max)

Levels: 1. Speed control using DC Motor Control Unit and measured using tachometer

2. Amplitude and input signal determined by the cam design

3) Secondary Mass

Levels: Adjusting secondary mass

7.2.5 Experiment No.5:

Objective: To measure the time response spring damper system with different current input to the damper.

Experimental Procedure: The damper is paired with two springs of stiffness 1.78 N/mm. It is then compressed to maximum compression and released. Time required to reach is measured.

CHAPTER 8
RESULTS AND DISCUSSION

8.1 Results for Experiment 1

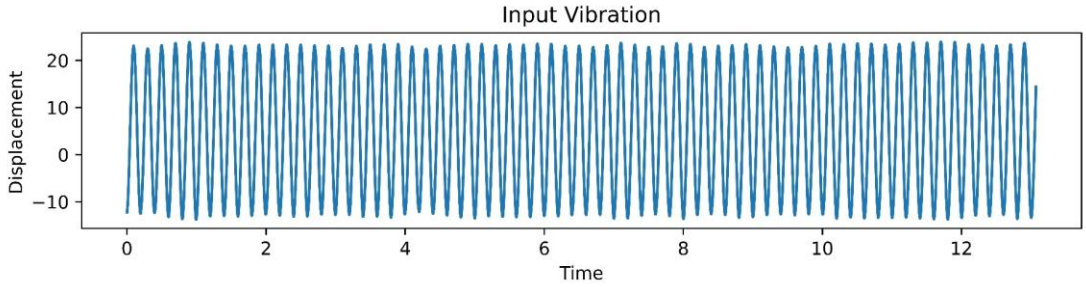

Fig 8.1 Sensor data obtained for 1.3 kg mass

The sensor data is obtained as below for each rpm. This is then processed using MATLAB code (Annexure I) and the amplitude vs Frequency graph is obtained.
A simple fft plot for one reading is

Maximum amplitude is observed at 8.71 Hz. The theoretical calculation was for a system with 8.33 Hz. Thus, natural frequency is similar to theoretical calculations.

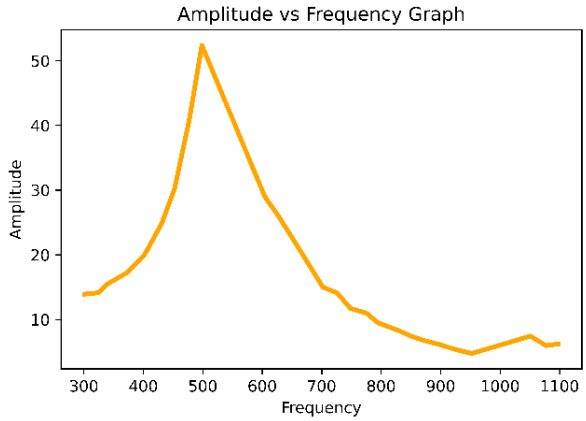

Fig 8.2 Experimental Frequency response plot for 1.3 kg

8.2 Results for Experiment 2

The sensor data is obtained as below for each rpm. This is then processed using Matlab code and the amplitude vs Frequency graph is obtained.

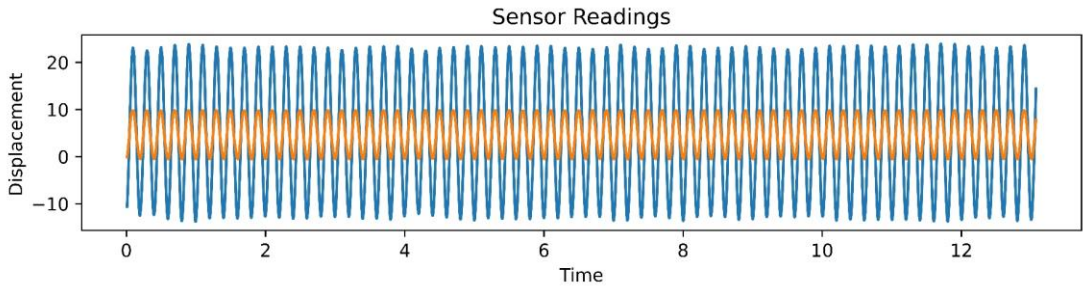

Fig 8.3 Sensor data obtained for 1.3 kg mass with vibration neutralizer

8.3 Results for Experiment 3

The MR damper is tested by using an Universal Testing Machine (UTM). The force applied on the damper is in downward motion and the experiment is performed with different input values of current. Input current applied on the damper are from 0 to 1 Ampere. This data can then be used to improve the control algorithm

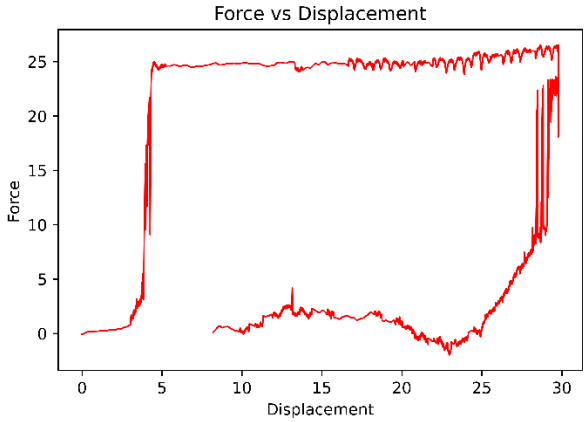

Fig 8.4 Force vs Displacement graph of the Damper at 0.6 A

The data thus obtained for each current was combined and fitted into bingham model obtained from literature.

The bingham model is as follows:

$$F = c_0\dot{x} + k_0 x + \alpha z + f_0$$

$$z = \tanh(\beta\dot{x} + \delta sign(x))$$

And the coefficients are expressed according to the current input as:

$$c_0 = c1 + c2 \times I + c3 \times I^2 + c4 \times I^3$$

$$k_0 = k1 + k2 \times I + k3 \times I^2 + k4 \times I^3$$

$$\beta = \beta 1 + \beta 2 \times I + \beta 3 \times I^2 + \beta 4 \times I^3$$

$$\delta = \delta 1 + \delta 2 \times I + \delta 3 \times I^2 + \delta 4 \times I^3$$

$$f_0 = f1 + f2 \times I + f3 \times I^2 + f4 \times I^3$$

Parameter	**Value**	**Parameter**	**Value**
$\boldsymbol{c1}$	-31.1678	$\beta 1$	-286.826
$\boldsymbol{c2}$	385.6730	$\beta 2$	273.573
$\boldsymbol{c3}$	-880.382	$\beta 3$	1324.245
$\boldsymbol{c4}$	576.724	$\beta 4$	-1384.44
$\boldsymbol{k1}$	-1.021	$\delta 1$	-8.605
$\boldsymbol{k2}$	11.5656	$\delta 2$	75.592
$\boldsymbol{k3}$	-30.372	$\delta 3$	-72.554
$\boldsymbol{k4}$	22.203	$\delta 4$	-97.982
$\boldsymbol{\alpha}$	3.442	$f1$	15.486
$\boldsymbol{f2}$	-81.753	$f3$	238.786
$\boldsymbol{f4}$	-120.721		

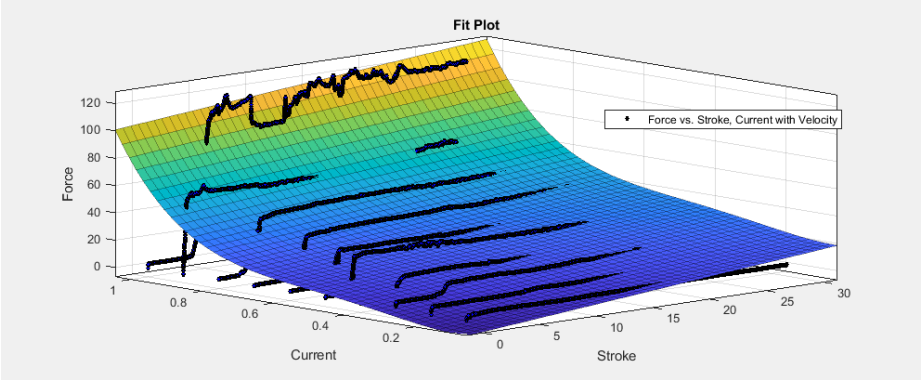

Fig 8.5 Damper function fitted to a graph

8.4 Results for Experiment 4

Data obtained for each rpm and each current is plotted in a frequency response plot as below.

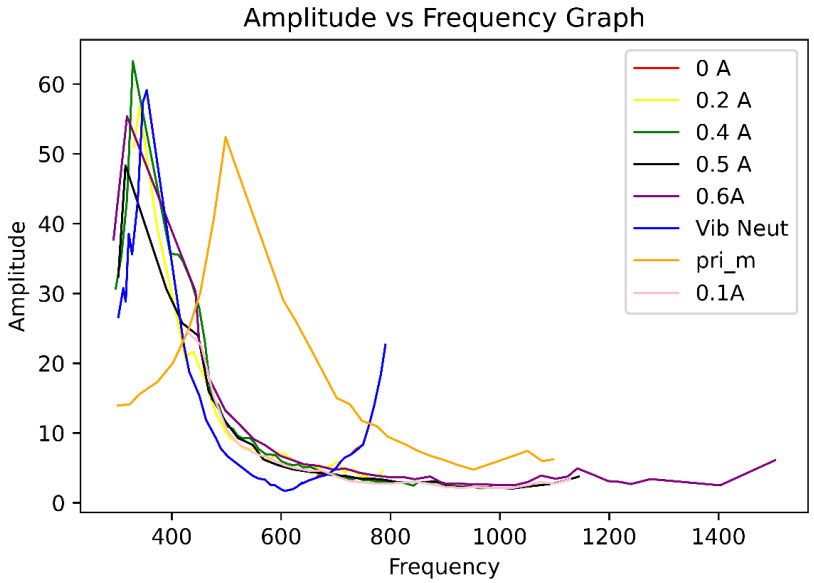

Fig 8.6 Amplitude vs Frequency curve for MRDVA at different currents

After reviewing the fig, it can be seen that at lower currents, the amplitude of vibration is higher at the same range of frequency. This amplitude reduces as we increase the current to higher values. This is because at higher values of current, the damper provides more damping force.

8.5 Results for Experiment 5

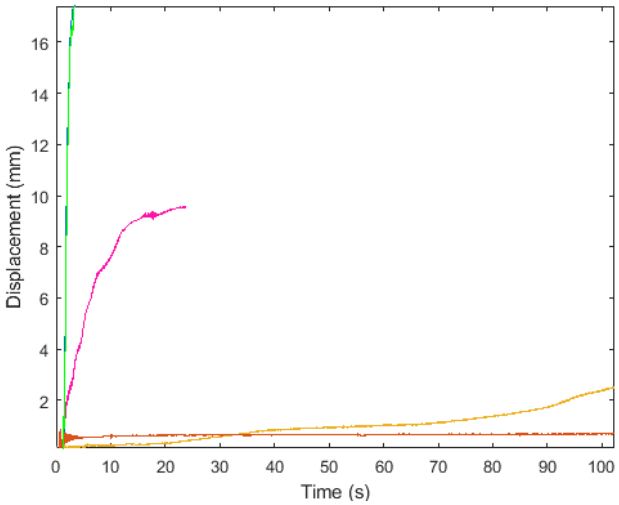

Fig 8.7 Time response of currents 0 A (blue), 0.1 A (green), 0.3A (pink), 0.4A (yellow) and 0.5 A (red).

This shows the time required to reach 3mm at each current. As is visible there is an exponential rise in response time. This should be taken into consideration while designing the control algorithm.

Table 8.1 Response time for different currents

Current to Damper	Time required to move 3mm
0A	1.58825
0.1 A	1.611
0.3 A	3.2475
0.4 A	128.1

8.6 INFERENCES FROM RESULTS FOR MRDVA

From Fig 8.6, it is clear that the designed MRDVA is effective in attenuating the vibration of the primary mass. The designed MRDVA system helps in reducing the peak formed due to resonance by the primary mass (without MRDVA). The MRDVA proves to be more

effective than a passive DVA, as it forms only one peak when compared to the two peaks formed by the passive DVA system. Increasing the current helps in reducing the amplitude of vibration produced. This is because the damping force provided by the damper is higher at higher currents.

The main working region of the MRDVA is from 10 to 18 Hz as observed from the graph above. Table 8.2 below shows the amplitude given by each current in this range.

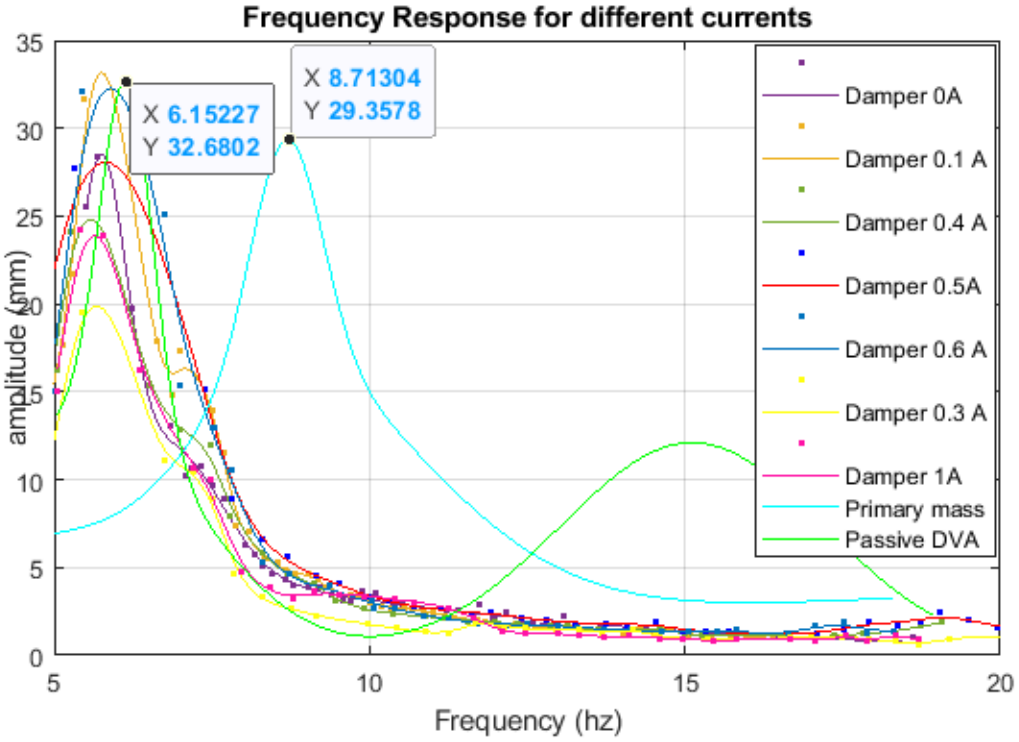

Fig 8.8 Amplitude (mm) vs frequency (rpm) graph of m1 = 1.3 kg and m2 = 0.9 kg

Table 8.2 Amplitude of vibration at different frequency and input currents

Frequency:	**10**	**11**	**12**	**13**	**14**	**15**
0 A	3.151	2.686	2.286	1.937	1.642	1.389
0.1 A	3.04671	2.445	1.795	1.523	1.329	1.277
0.3 A	1.768	1.306	1.737	1.436	1.395	0.979
0.4 A	2.60405	2.1775	1.885	1.663	1.475	1.247
0.5 A	3.39746	2.653	2.331	1.932	1.774	1.488

0.6 A	3.01729	2.213	1.785	1.651	1.454	1.35
1 A	3.355	2.877	1.578	1.21	1.078	0.905
SDOF	15.017	10.5732	7.26	4.962	3.674	3.135
Vibration neutralizer	1.084	1.835	4	7.253	10.494	12.085

Table 8.3 Best current to tune Damper and the reduction it provides

Frequency (Hz)	**Best current**	**% Decrease wrt primary mass alone**	**% Decrease wrt passive DVA**
10	Passive	92.7%	-
11	0.3 A	87.65%	28.8%
12	1 A	78.26%	60.55%
13	1 A	75.6%	83.3%
14	1 A	70.65%	89.7%
15	1 A	71.13%	92.5%
16	1 A	70.1%	91.92%
17	0 A	69.7%	88.48%
18	0 A	74.23%	82.3%

This result can be used to develop a control algorithm for MR Damper. The system would require a sensor that measures frequency, and then the corresponding optimal current could be obtained to minimize vibration.

The study was also conducted with different sets of masses to see its applicability for different mass ratios. The results are as below.

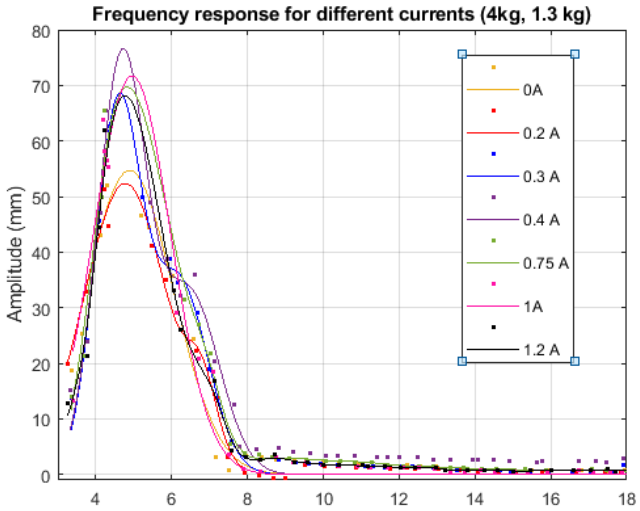

Fig 8.9 Amplitude (mm) vs frequency (rpm) graph of m1 = 4 kg and m2 = 1.3 kg

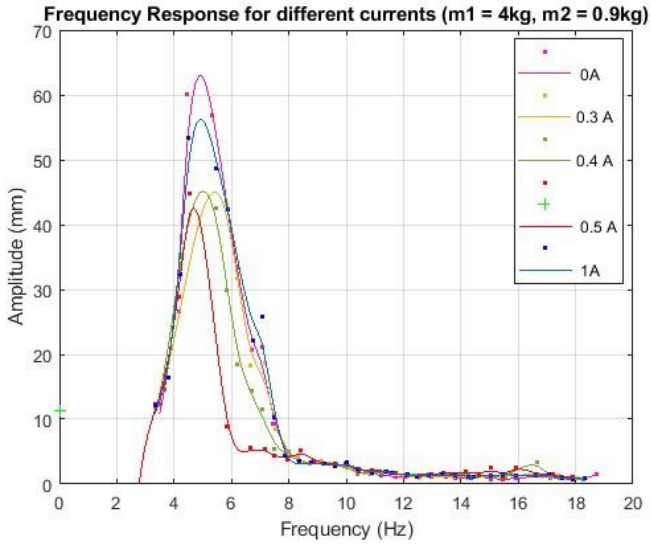

Fig 8.10 Amplitude (mm) vs frequency (rpm) graph of m1 = 4 kg and m2 = 0.9 kg

8.7 ADDITIONAL RESULTS

Dynamic Vibration Absorber as a Vibration Neutralizer

The DVA system is designed such that in case of there is no MR Damper, the system minimizes the natural frequency of primary system. In order to understand vibration neutralizer properties, we require its amplitude vs frequency. This helps us understand the effectiveness of the device. The amplitude vs frequency plots were obtained both theoretically and experimentally. The experimental results were then compared to the theoretical results. After validating the experimental results using the theoretical results,

amplitude vs frequency plots for the system with and without the neutralizer were compared to check whether the neutralizer is effective in reducing vibrations.

Here, we have taken a primary mass of 1.3 Kg and a secondary mass of 0.9 Kg. The corresponding mass ratio was found to be 0.692. The amplitude vs frequency curves for the same have been plotted both experimentally and theoretically, and has been shown in Fig 8.11.

The passive DVA or the vibration neutralizer has eliminated the natural frequency. We can also see that it matches well with the theoretical design of the passive DVA as seen in Fig 8.12.

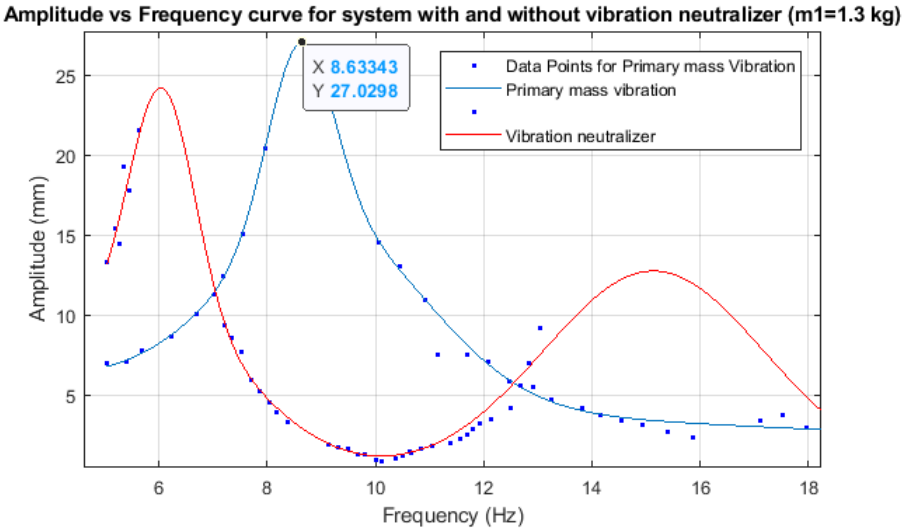

Fig 8.11 Experimental Amplitude vs Frequency Plots for system with and without Vibration Neutralizer ($m_1 = 1.3Kg, m_2 = 0.9Kg$)

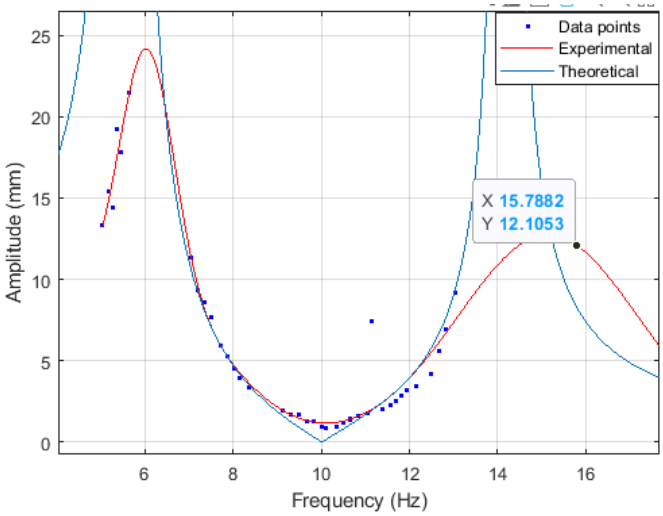

Fig 8.12 Theoretical and Experimental Amplitude vs Frequency Plots ($m_1 = 1.3Kg, m_2 = 0.9Kg$)

CHAPTER 9

ADDITIONAL WORK DONE

9.1 SELF AGITATOR PISTON

When choosing a suitable MR Fluid, a tradeoff is often necessary between the strength of magneto-rheological properties and resistance to settling as larger particles give better MR properties but increase chances of settling. The chosen MR Fluid in this experiment is proven to be resistant to hard settling but is still prone to a loss of homogeneity over longer periods of time. This can be solved by mixing the fluid which might not be possible when it is implemented in a system. A simple stirrer mechanism can provide a twisting movement along with downward compression. The angle of rotation to compression ratio is kept low to avoid undesirable forces in the damper

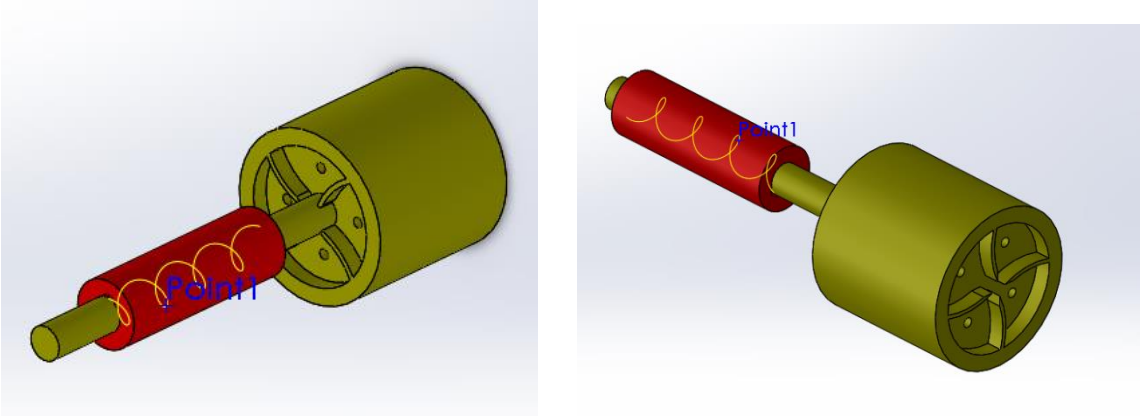

Fig 9.1 : Back view and front view of self agitator piston

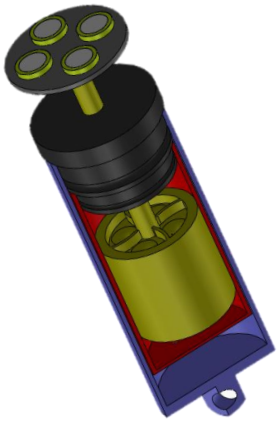

Fig 9.2 : Self Agitator Piston incorporated in the damper

9.2 ENERGY HARVESTER

One of the aims of this project is to make the DVA energy efficient. External energy is required to power the MR damper and its corresponding Controllers. To this end, energy harvesting methods were studied that could convert energy from the vibrations to energy usable by the MR Damper. Some of these methods are mentioned below.

9.2.1 Electro-Magnetic Induction

A permanent magnet is located at the end of the piston surrounded by induction coils. As the piston moves back and forth, it induces a current in the coil. The magnetic field produced by the permanent magnet has minimal influence on the regions of interest in the Primary piston.

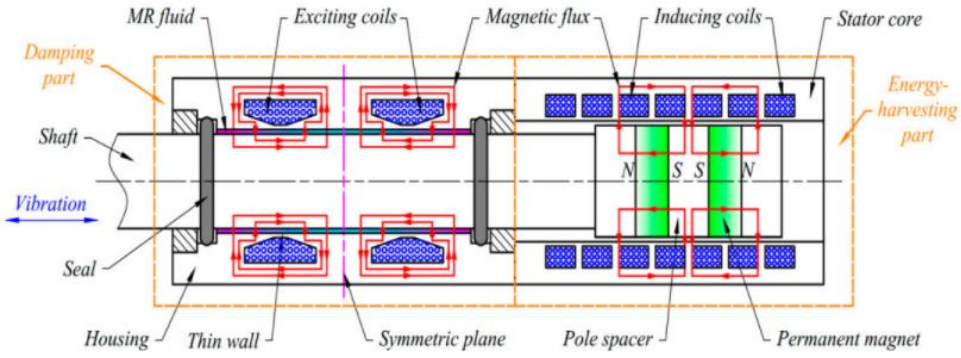

Fig 9.3 Schematic of the proposed self-powered shear-mode magnetorheological (MR) damper

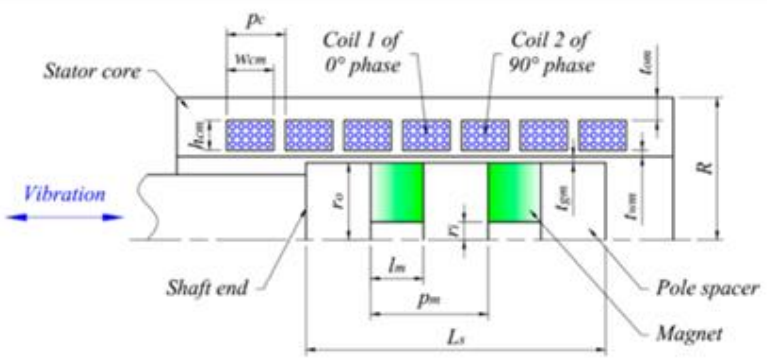

Fig 9.4 Schematic diagram of Energy Harvester component

9.2.2 Piezo Electric Method

Piezoelectric materials are materials that can generate internal electrical charges from applied mechanical stress. Designing an energy harvester in which some stress is imparted to the piezoelectric material provides an energy harvesting method. There are two ways to go about this, as mentioned below.

Cymbal type

In this method, the interface of the DVA and primary mass is lined with cymbal type piezoelectric transducers. The force by the vibration of primary mass is converted to useable energy.

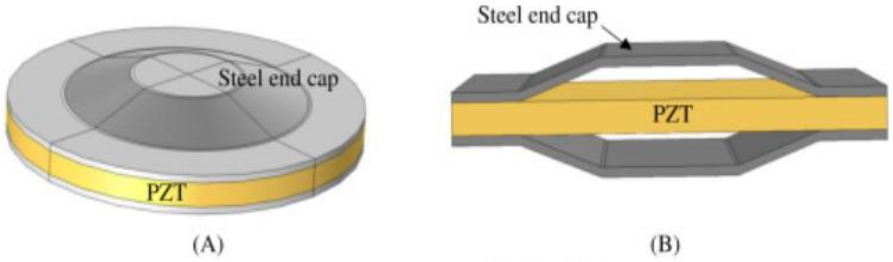

Fig 9.5 Illustration of PZT transducers for (A) cymbal, (B) bridge

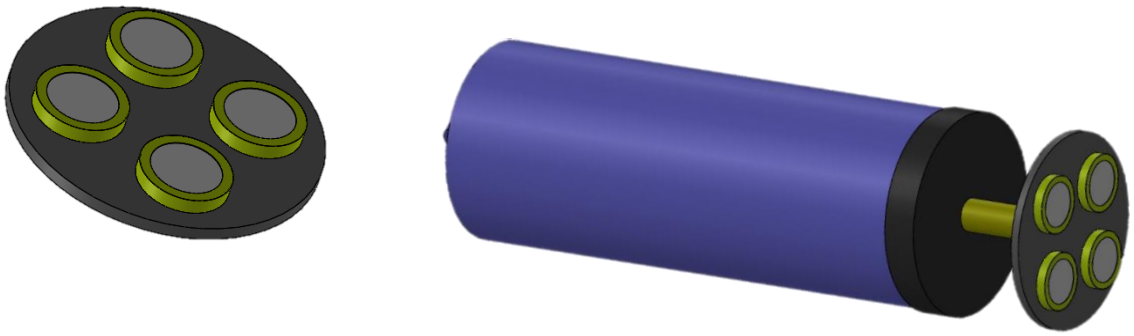

Fig 9.6 The CAD model of prototype for the application of the EH and its location

Fig 9.7 Front view and right-hand side view of assembly of MR Damper

Cantilever Type

As shown in Fig 9.8, the system consists of a vibrating piezoelectric bimorph cantilever with an attached mass and two permanent magnets: one serving as the end mass and the other attached to the bottom of the ferromagnetic fluid holder.

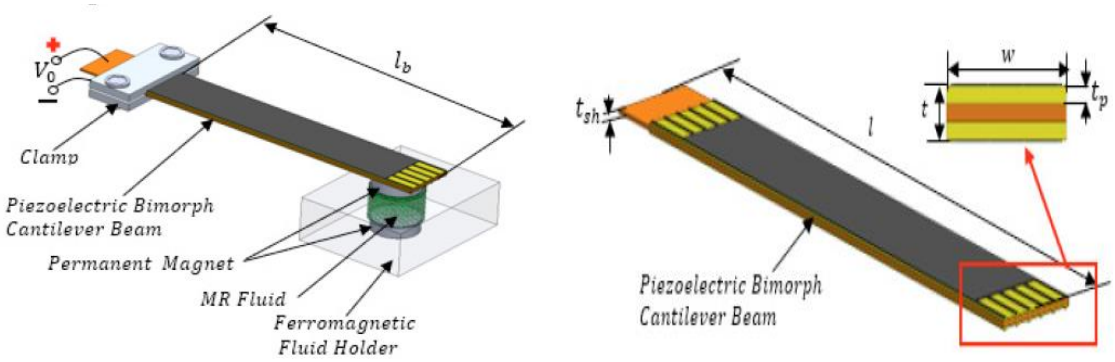

Fig. 9.8 Schematic diagram of the proposed variable-damping MR fluid energy harvester

In order to provide means of transferring the linear motion of the piston rod without transferring the rotational motion a mechanism was designed as shown in Fig 9.9.

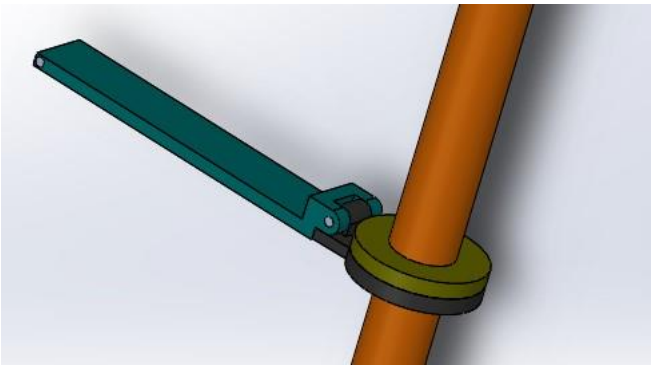

Fig 9.9 CAD model of mechanism designed to attached to the piston rod

CHAPTER 10

CONCLUSIONS AND SCOPE OF WORK

10.1 CONCLUSION

The aim of the project is to design and optimize a semi-active Dynamic Vibration Absorber which uses MR Fluid technology. A mathematical model of a passive DVA, as well as an MR-DVA, was created. This was backed up by a fluid simulation of the MR Damper. According to the simulations and design, an MR-DVA was fabricated. The characteristics of the fabricated DVA correspond to the theoretical model. The results of these experiments conducted on the MR-DVA show the passive DVA removes high amplitude at natural frequency but gives two other peaks. Passive DVA can thus be used for eliminating a particular frequency to which it is tuned. Using the MR Damper allowed us to eliminate one of the peaks and improve the range of working of the MR DVA. The ideal current input to obtain lowest amplitudes at different frequencies was noted and this can be used as a control algorithm to adjust the current input automatically.

10.2 SCOPE FOR FUTURE WORK

- Synthesis of the MR fluids with varied composition and their characterization. Optimising composition for required damping properties.
- Fabricating a customized damper for our application based on simulation results.
- Combining theoretical model and experimental data to develop an optimized control system.
- Implementing the innovations like stirrer in a customized damper

APPENDIX I

Matlab code for obtaining amplitude vs Frequency graph from all the files in a folder.

```
inputdir = 'D:\ Experimentation\4 kg 0.9 kg\4KG without Damper'
Damper4kgneutr= zeros;

S = dir(fullfile(inputdir,'*.csv'));
for k = 1:numel(S)-1
    fnm = fullfile(inputdir,S(k).name);
    %txt = load(fnm);
    %% Import data from text file.
    % Script for importing data from the following text file:
    %
    %    D:\Major Project\Experimentation\310_base_pri2022-03-29
16.50.29.010_A0000.csv
    %
    % To extend the code to different selected data or a different text
file, generate a function instead of a script.

    % Auto-generated by MATLAB on 2022/04/07 15:45:09

    %% Initialize variables.
    filename = fnm;
    startRow = 6;

    %% Read columns of data as text:
    % For more information, see the TEXTSCAN documentation.
    formatSpec = '%15s%12s%s%[^\n\r]';

    %% Open the text file.
    fileID = fopen(filename,'r');

    %% Read columns of data according to the format.
    % This call is based on the structure of the file used to generate
this code. If an error occurs for a different file, try regenerating the
code from the Import Tool.
    textscan(fileID, '%[^\n\r]', startRow-1, 'WhiteSpace', '',
'ReturnOnError', false, 'EndOfLine', '\r\n');
    dataArray = textscan(fileID, formatSpec, 'Delimiter', '',
'WhiteSpace', '', 'TextType', 'string', 'ReturnOnError', false);

    %% Close the text file.
```

```
    fclose(fileID);

    %% Convert the contents of columns containing numeric text to numbers.
    % Replace non-numeric text with NaN.
    raw = repmat({''},length(dataArray{1}),length(dataArray)-1);
    for col=1:length(dataArray)-1
        raw(1:length(dataArray{col}),col) = mat2cell(dataArray{col},
ones(length(dataArray{col}), 1));
    end
    numericData = NaN(size(dataArray{1},1),size(dataArray,2));

    for col=[1,2,3]
        % Converts text in the input cell array to numbers. Replaced non-
numeric text with NaN.
        rawData = dataArray{col};
        for row=1:size(rawData, 1)
            % Create a regular expression to detect and remove non-numeric
prefixes and suffixes.
            regexstr = '(?<prefix>.*?)(?<numbers>([-
]*(\d+[\,]*)+[\.]{0,1}\d*[eEdD]{0,1}[-+]*\d*[i]{0,1})|([-
]*(\d+[\,]*)*[\.]{1,1}\d+[eEdD]{0,1}[-+]*\d*[i]{0,1}))(?<suffix>.*)';
            try
                result = regexp(rawData(row), regexstr, 'names');
                numbers = result.numbers;

                % Detected commas in non-thousand locations.
                invalidThousandsSeparator = false;
                if numbers.contains(',')
                    thousandsRegExp = '^[-/+]*\d+?(\,\d{3})*\.{0,1}\d*$';
                    if isempty(regexp(numbers, thousandsRegExp, 'once'))
                        numbers = NaN;
                        invalidThousandsSeparator = true;
                    end
                end
                % Convert numeric text to numbers.
                if ~invalidThousandsSeparator
                    numbers = textscan(char(strrep(numbers, ',', '')),
'%f');
                    numericData(row, col) = numbers{1};
                    raw{row, col} = numbers{1};
                end
            catch
                raw{row, col} = rawData{row};
            end
        end
    end
```

```
    %% Replace non-numeric cells with NaN
    R = cellfun(@(x) ~isnumeric(x) && ~islogical(x),raw); % Find non-
numeric cells
    raw(R) = {NaN}; % Replace non-numeric cells

    %% Create output variable
    basepri1 = table;
    basepri1.ProtocolTimest = cell2mat(raw(:, 1));
    basepri1.ampSensor = cell2mat(raw(:, 2));
    basepri1.Distance0SensorDistance1 = cell2mat(raw(:, 3));

    %% Clear temporary variables
    clearvars filename startRow formatSpec fileID dataArray ans raw col
numericData rawData row regexstr result numbers invalidThousandsSeparator
thousandsRegExp R;


    K = basepri1.ampSensor;
    X = basepri1.Distance0SensorDistance1;
    T = basepri1.ProtocolTimest(2)-basepri1.ProtocolTimest(1);
% Sampling period
    Fs = 1/T;            % Sampling frequency
    L = length(X);             % Length of signal
    t = (0:L-1)*T;        % Time vector

    %plot(t(1:L),X(1:L))
    %title('signal')
    %xlabel('t (seconds)')
    %ylabel('X(t)')

    Y = fft(X);

    P2 = abs(Y/L);
    P1 = P2(1:L/2+1);
    P1(2:end-1) = 2*P1(2:end-1);


    f = Fs*60*(0:(L/2))/L;
    plot(f,P1)
    %title('Single-Sided Amplitude Spectrum of X(t)')
    %xlabel('f (Hz)')
    %ylabel('|P1(f)|')


    [a1,a2] = max(P1);
    a3 =f(a2);
    if a3==0
        [a1,a2] = max(P1(1:end ~= a2));
```

```
        a3 = f(a2);
    end
    Damper4kgneutr(k,1) = (max(K)-min(K))/2;
    Damper4kgneutr(k,2) = a3;
end


plot(Damper4kgneutr(:,2),Damper4kgneutr(:,1),'.');
```

APPENDIX II

Matlab code for plotting theoretical frequency response curve

```
k1 = 1612.2*2;
m1 = 4;
m2 = 0.9;
k2 = (1.8095+1.7541)*1000;
mu = m2/m1;
w_a = sqrt(k2/m2);
w_n = sqrt(k1/m1);
f  = w_a/w_n;
cc = 2*w_n*m2;
c2  = 0.028;
eeta = c2/cc;


M = zeros;
Q = zeros;




for i = 1 : 5001
w_wn(i) = 50 * (i-1)/1000;
Q(i) = w_wn(i)/w_n;



M(i) = sqrt((((2*eeta*Q(i))^2)+((Q(i)^2-
f^2)^2))/(((2*eeta*Q(i))^2)*((Q(i)^2-1+mu*(Q(i)^2))^2)+(mu*(f^2)*(Q(i)^2)-
(Q(i)^2-1)*(Q(i)^2-f^2))^2));
end;


plot(w_wn/(2*pi), M*9.3);
hold on;
```

```
xlabel ('Frequency (Hz)');
ylabel('Tr');
 xlim([200/60 1200/60])
 ylim([0 40])
%%gtext('zeta = 0.1');
%gtext('zeta = 0.2');
%gtext('zeta = 0.3');
%gtext('zeta = 0.4');
%gtext('zeta = 0.5');
title('Ex9.2');
grid on;
hold on
```

APPENDIX III

Matlab code for fitting non linear curve in MR Damper equation

```
% Create an anonymous function that describes the expected relationship
% between X and Y
f=@(c,x) x(:,2).*(c(1)+c(10)*(x(:,3))+c(11)*(x(:,3).^2)+c(12)*(x(:,3).^3))
+ x(:,1).*(c(2)+c(13)*(x(:,3))+c(14)*(x(:,3).^2)+c(15)*(x(:,3).^3)) +
(c(3))*atan(c(8)*x(:,2)+c(9)*sign(x(:,2)))
+c(4)+c(5)*(x(:,3))+c(6)*(x(:,3).^2)+c(7)*(x(:,3).^3);
% data set
% Specify x variables from data file,Re,Theta and Beta columns.
x=Total;
% Specify y variable from data file ,(Nu)column.
y=Force;
% Specify a vector of starting conditions for the solvers
c0=[100;100;100;1;1;100;1;1;1;1;1;1;1;1;1;];
% Perform a nonlinear regression
Beta=nlinfit(x,y,f,c0)
```

REFERENCES

1. T. G. Lazareva and G. Shitik, "Magnetic and magnetorheological properties of flowable compositions based on barium and strontium ferrites and iron oxide", Proceedings of SPIE Conference on Smart Structures and Materials: Passive Damping and Isolation, SPIE Vol. 3045, 1997
2. O. Ashour, D. Kinder, V. Giurgiutiu, and C. Roger, "Manufacturing and characterization of magnetorheological fluids", Proceedings of SPIE Conference on Smart Structures and Materials: Smart Materials Technologies, 1996
3. O. Ashour, C. A. Rogers, and W. Kordonsky, "Magnetorheological fluids: materials characterization, and devices", Journal of Intelligent Material Systems and Structures, Vol. 7, 1996.
4. Kolekar S, Venkatesh K, Oh J-S, Choi S-B, “Vibration controllability of sandwich structures with smart materials of electrorheological fluids and magnetorheological materials: a review.” J Vib Eng Technology
5. J. D. Carlson, D. M. Catanzarite, and K. A. St. Clair, "Commercial Magnetorheological fluid devices", International Journal of Modern Physics B, Vol. 10, 1996
6. W. Kordonsky, "Elements and devices based on magnetorheological effect", Journal of Intelligent Materials, Systems and Structures, Vol. 4, 1993
7. R. Bolter and H. Janocha, "Design rules for MR fluid actuators in different working modes", Proceedings of SPIE Conference on Smart Structure.
8. J.D. Carlson, M. J. Chrzan, “Magnetorheological fluid dampers”, US Patent US5277281A, 1994
9. J. D. Carlson, M. J. Chrzan, F. O. James “Magnetorheological fluid devices”, US Patent, US5284330A, 1994
10. D Karnopp, M. J. Crosby, Harwood RA “Vibration control using semi-active force generators” 96 Ser B:619–626
11. T Kobori, S Kamagata, “Active variable stiffness system— active seismic response control”, The US–Italy–Japan Workshop/Symposium on Structural Control and Intelligent Systems, Sorrento, Italy, 1992

12. Yoshida O, Dyke S J, “Seismic control of a nonlinear benchmark building using smart dampers” Journal of Engineering Mechanics, Vol 130, 2004
13. D.A. Pohoryles, P Dufour, “Adaptive control of structures under dynamic excitation using magnetorheological dampers: an improved clipped-optimal control algorithm” Journal of Vibration Control, Vol 21, 2015
14. D. L. Margolis, "The response of active and semi-active suspensions to realistic feedback signals". Vehicle System Dynamics, Vol. 11, 1982
15. S. Hwang, S. Heo, H. Kim, and K. Lee, "Vehicle dynamic analysis and evaluation of continuously controlled semi-active suspensions using hardware-in-the-loop simulation", Vehicle System Dynamics, Vol. 27, 1997.
16. A. Titli, S. Roukieh, and E. Dayre, "Three control approaches for the design of car semi-active suspension", Proceedings of the 32nd IEEE Conference on Decision and Control, Vol. 3, 1993.
17. R. A. Decarlo, S. H. Zak, and G. P. Matthews, "Variable structure control of nonlinear multivariable systems: a tutorial", Proceedings of the IEEE, Vol. 76 (3), 1988.
18. H. S. Lee, S. Bok Choi, “Control and response characteristics of a magneto-rheological fluid damper for passenger vehicles”, Journal of Intelligent Material Systems and Structures, Vol 11, 2000
19. B. Kasemi, A. G. A. Muthalif , M. M. Rashid, S. Fathima, “Fuzzy-PID controller for semi-active vibration control using magnetorheological fluid damper”, Procedia Engineering, Vol 41, 2012
20. O. Erol, B. Gonenc, D. Senkal, S. Alkan, H. Gurocak, “Magnetic induction control with embedded sensor for elimination of hysteresis in magnetorheological brakes”, Journal of Intelligent Material Systems and Structures, Vol 23, 2012
21. C. Ciocanel, M. H. Elahinia, K. E. Molyet, N. G. Naganathan, “Design analysis and control of a magnetorheological fluid based torque transfer device”, International Journal of Fluid Power, Vol 9, 2008
22. O. Jong-Seok, C. Seung-Hyun, C. Seung-Bok, “Design of a 4-DOF MR haptic master for application to robot surgery: virtual environment work”, Smart Materials and Structures, Vol 23, 2014

23. M. Yokoyama, J. Karl Hedrick, S. Toyama, " A model following sliding mode controller for semi-active suspension systems with MR dampers", Proceedings of the American Control Conference, 2001
24. R. K. Dixit, G. D. Buckner, "Sliding mode observation and control for semi active vehicle suspensions", Vehicle System Dynamics: International Journal of Vehicle Mechanics and Mobility, Vol 43, 2005
25. L. Y. Li, G. Song, J. P. Ou, "Observer and controller design for vibration suppression of a structure with MR brakes as nonlinear hinges", Earth and Space 1-10 doi: 10.1061/40988(323)203
26. D. X. Phu, N. Vien Quoc, P. Joon-Hee, C. Seung-Bok, "Design of a novel adaptive fuzzy sliding mode controller and application for vibration control of magnetorheological mount", Proceedings of the Institution of Mechanical Engineers, Part C: Journal of Mechanical Engineering Science, 2014
27. S. B. Kumbhar, S. P. Chavan, S. S. Gawade, "Two Way Stiffness Tuning of Magneto-rheological Elastomer-Shape Memory Alloy Composite," Materials today Proceedings, Vol. 5(5), 2018
28. S. B. Kumbhar, S. P. Chavan, S.S Gawade, "Adaptive Tuned Vibration Absorber Based on Magneto-rheological Elastomer-Shape Memory Alloy Composite," Mechanical Systems and Signal Proc., Vol 100, 2018
29. L. Jin-Chein, M. H. Nien, "Adaptive Control of a Composite Cantilever Beam with Piezoelectric Damping-Modal Actuators/Sensors," Journal of Composite Structures, Vol 70, 2005
30. Z. Parlak, T. Engin, I. Çalli, "Optimal design of MR damper via finite element analyses of fluid dynamic and magnetic field", Elsevier - Mechatronics, Vol 22, 2012
31. A. Roszkowski, M. Bogdan, W. Skoczynski, B. Marek, "Testing Viscosity of MR Fluid in Magnetic Field", Measurement Science Review, Vol 8, 2008
32. D. Grivon, "Design, Modelling and Sensing Possibilities of Magneto-Rheological Based Devices", Doctoral dissertation, École Polytechnique Fédérale De Lausanne, 2017